

ABSTRACT

Title of Thesis: Characterization of programmed -1 ribosomal frameshift signals in the interleukin 2 receptor gamma mRNA

Zachary Robert Flickinger, Master of Science, 2016

Thesis Directed By: Professor and Chair, Jonathan Dinman, Department of Cell Biology and Molecular Genetics

Programmed -1 ribosomal frameshift (-1 PRF) signals are predicted to be present in ~10% of eukaryotic mRNA, suggesting a conserved role for -1 PRF in eukaryotic mRNA translation. This work focuses on -1 PRF in the interleukin 2 receptor gamma (IL2RG) mRNA. IL2RG is a component of receptors for six cytokines responsible for lymphocyte proliferation and differentiation. Altered expression of IL2RG is linked to immunodeficiency and lymphoma. We verified that the IL2RG mRNA has one potential -1 PRF signal in exon 3 that stimulates -1 frameshifting and a second in exon 8 that is definitively a -1 PRF signal. Both of these signals redirect the ribosome to a premature termination codon, suggesting -1 PRF alters IL2RG expression via NMD. Testing the effect of cancer patient associated mutations discovered in

the exon 8 -1 PRF signal may elucidate a role for IL2RG -1 PRF in normal physiology and pathological phenotypes.

CHARACTERIZATION OF PROGRAMMED -1 RIBOSOMAL FRAMESHIFT
SIGNALS IN THE INTERLEUKIN 2 RECEPTOR GAMMA MRNA

by

Zachary Robert Flickinger

Thesis submitted to the Faculty of the Graduate School of the
University of Maryland, College Park, in partial fulfillment
of the requirements for the degree of
Master of Science
2016

Advisory Committee:
Professor Jonathan Dinman, Chair
Professor Anne Simon
Associate Professor Eric Haag

© Copyright by
Zachary Robert Flickinger
2016

Acknowledgements

I have benefitted immensely from the supportive and enjoyable work environment that all the Dinman lab members have provided. I would like to thank my committee members for their time and critical input. I especially want to thank Jon for his encouragement to pursue my interests and his advice on work and life. I would also like to thank Maria for all of her encouragement during long nights of writing and my parents for their love and support.

This work was supported by the NIH grant RO1GM117177 awarded to Jonathan Dinman and the “Training Program in Cell and Molecular Biology” T32 GM080201 grant awarded to myself.

Table of Contents

Acknowledgements	v
Table of Contents	vi
List of Tables	viii
List of Figures	ix
List of Abbreviations	x
Chapter 1: Introduction	1
Establishment of reading frame	2
Programmed -1 Ribosomal Frameshifting.....	4
Nonsense-mediated decay pathway	9
Potential role of -1 PRF regulation on IL2RG expression	12
Chapter 2: Results.....	17
The IL2RG -1 PRF signal at 354 promotes efficient -1 frameshifting	17
Disrupting the slip site affects -1 frameshift efficiency of the IL2RG 1008 -1 PRF signal	18
The IL2RG -1 PRF signal at 1008 induces -1 frameshifting at the slip site	18
Mutations in the IL2RG 1008 -1 PRF signal are present in cancer patients	22
Chapter 3: Discussion	26
Chapter 4: Materials and methods.....	30
Plasmid construction.....	30
Yeast transformations	34
β -galactosidase (β -GAL) assay.....	35

Mammalian cell culture	36
Mammalian cell transfections.....	37
-1 PRF dual-luciferase assays	38
Production and purification of IL2RG -1 PRF:: β -GAL fusion protein from yeast	39
In-gel digestion of IL2RG -1:: β -GAL and peptide extraction.....	41
LC-MS/MS analysis of IL2RG -1PRF:: β -GAL fusion protein	41
LC-MS/MS data analysis.....	42
Appendix A: Table of oligonucleotides used for cloning, sequencing primers, and qPCR primers.....	43
Appendix B: Table of plasmids made or used.....	51
Appendix C: Table of yeast strains made or used.....	56
Appendix D: Table of hotknots folding solutions for mammalian sequences that align with Homo sapiens IL2RG -1 PRF signal at 354.	61
Appendix E: Table of nupack solutions for mammalian sequences that align with Homo sapiens IL2RG -1 PRF signal at 1008.....	63
Bibliography.....	65

List of Tables

Table 1. Cancer associated SNPs tested in dual luciferase reporter.....	24
Table 2. Oligonucleotides used for cloning, sequencing primers, and qPCR primers	43
Table 3. Plasmids made or used	51
Table 4. Yeast strains made or used	56
Table 5. Hotknots folding solutions for mammalian sequences that align with <i>Homo sapiens</i> IL2RG -1 PRF signal at 354.....	61
Table 6. Nupack solutions for mammalian sequences that align with <i>Homo sapiens</i> IL2RG -1 PRF signal at 1008.	63

List of Figures

Figure 1. Basic structure of the ribosome.	2
Figure 2. Structure of a typical -1 PRF signal.	5
Figure 3. -1 PRF may occur through multiple kinetic partitioning pathways. ...	8
Figure 4. Two models of nonsense-mediated decay (NMD) pathway.	11
Figure 5. Predicted structure of IL2RG -1 PRF at 1008 and ribosome profiling data of IL2RG mRNA.....	13
Figure 6. Predicted structures of a -1 PRF signal at position 354 of IL2RG mRNA.....	14
Figure 7. % -1 frameshifting of IL2RG -1 PRF signals in HeLa cells (A) and HEK293T cells (B).	18
Figure 8. LC-MS/MS sequence coverage of IL2RG@1008:: β -GAL.	20
Figure 9. Table of all trans-frame peptides sequenced by LC-MS/MS.	21
Figure 10. Mass spectrum of the IL2RG -1 PRF at 1008 trans-frame peptide.	22
Figure 11. Patient mutations found in the IL2RG -1 PRF signal at 1008.	23
Figure 12. % -1 frameshifting of IL2RG -1 PRF signal at 1008 with cancer associated SNPs.	25
Figure 13. Alignment of metazoan IL2RG sequences to the Homo sapiens signal at 354.	57
Figure 14. Alignment of metazoan IL2RG sequences to the Homo sapiens signal at 1008.	59

List of Abbreviations

mRNA	messenger RNA
LSU	large ribosomal subunit
SSU	small ribosomal subunit
tRNA	transfer RNA
aa-tRNA	aminoacyl-tRNA
ORF	open reading frame
met-tRNA _i	initiator methionine-tRNA
eIF	eukaryotic initiation factor
PABP	poly-adenosine binding protein
eEF	eukaryotic elongation factor
eRF	eukaryotic release factor
GTP	guanosine triphosphate
-1 PRF	programmed -1 ribosomal frameshift
HIV-1	human immunodeficiency virus-1
SARS	severe acute respiratory syndrome
PTC	premature termination codon
NMD	nonsense-mediated decay
NSD	non-stop decay
NGD	no-go decay
uORF	upstream open reading frame
ATPase	adenosine triphosphatase
EJC	exon junction complex

SURF	UPF1-SMG1-eRF1-eRF3 complex
UTR	untranslated regions
mRNP	messenger ribonucleoprotein
NCBI	national center for bioinformatics
SCID	severe combined immunodeficiency
IL2RG	interleukin receptor 2 gamma chain
MFE	minimum free energy
SSSM	silent slip site mutant
β -GAL	β -galactosidase
ONPG	o-nitrophenyl- β -galactopyranoside
LC-MS/MS	liquid chromatography-tandem mass spectrometry
SNP	single nucleotide polymorphism
CMV	cytomegalovirus
ssDNA	single-stranded DNA
TE	Tris-EDTA
LiOAc	Lithium Acetate
SDS	sodium dodecyl sulfate
PBS	phosphate buffered saline
OD	optical density
DMEM	Dulbecco's modified Eagle's medium

Chapter 1: Introduction

A key step in the “central dogma” of biology is the translation of messenger RNA (mRNA) into protein.¹ Translation is performed by the ribosome.

Ribosomes are made up of two major subunits termed the large subunit (LSU) and small subunit (SSU). The SSU functions primarily as the decoding center of the ribosome, where mRNA and transfer RNA (tRNA) interactions occur.² The tRNA act as an intermediary between mRNA decoding and peptide synthesis. The primary function of the LSU is to catalyze peptidyl transfer.² Binding domains formed by the complex of both subunits are required for association with tRNA and accessory factors. These tRNA binding sites are described in figure 1.³

An important aspect of protein synthesis is that the ribosome translates the mRNA in groups of exactly three nucleotides at a time. These three nucleotides, termed a codon, are translated into a single amino acid.⁴ This amino acid is delivered to the ribosome by an aa-tRNA with a matching anticodon sequence that base pairs with the mRNA codon. Since the mRNA is decoded three bases at a time it gives the ribosome the capacity to translate three separate reading frames. Only one of these reading frames, termed the open reading frame (ORF), is translated into a functional protein in canonical eukaryotic translation. However, organisms have evolved to utilize more than one reading frame in order to add an additional layer of regulation to protein expression. To understand how the three reading frames can be

manipulated to regulate protein expression, it is important to first describe the basis for how reading frame is established and maintained.

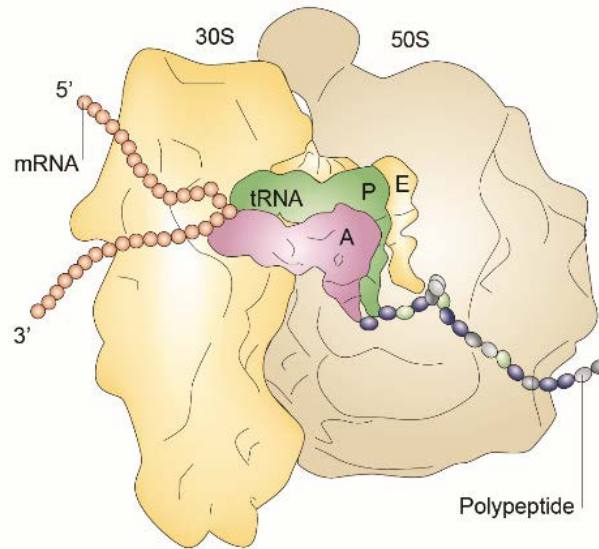


Figure 1. Basic structure of the ribosome.

The large and small subunits form three binding domains for tRNA termed the A, P, and E sites. The A site of the ribosome is defined as the site of all aminoacylated-tRNA (aa-tRNA) binding, except for the initiator methionine-tRNA (met-tRNA_i) which binds to the P site of the ribosome. During ribosomal elongation the peptidyl-tRNA occupies the P site. The elongating polypeptide chain is extruded from the peptidyl transferase center through an exit tunnel in the LSU. Figure adapted from source 3.

Establishment of reading frame

The ribosome established reading frame during the initiation step of translation. Canonical eukaryotic translation initiation requires covalent modifications to the mRNA; these covalent modifications include addition of a 5' 7-methylguanylate triphosphate cap, splicing (unless the mRNA has no introns to splice out), and polyadenylation of the 3' end.⁵ The mature mRNA is

bound by the eukaryotic initiation factor 4F (eIF4F) complex at the 5' cap and by the poly-adenosine binding protein (PABP) at the polyadenylated 3' end. At this point the 43S pre-initiation complex (PIC), consisting of the SSU, initiation factors, and the met-tRNA_i, interacts with the eIF4F complex and starts scanning the mRNA for a translation start site.^{6,5} The translation start site in eukaryotes is defined as an AUG codon flanked by a consensus Kozak sequence.⁷ Once the met-tRNA_i binds to a start codon the LSU is recruited to the start site and translation elongation begins.⁸

Maintenance of reading frame

After initiating at an AUG start codon the ribosome must maintain the same reading frame in order to synthesize the intended protein during elongation. This requires specific interactions between the ribosome, accessory factors, aa-tRNA, and the mRNA. Addition of a new amino acid to the elongating peptide chain starts with base pairing between an incoming aa-tRNA anticodon and the mRNA codon in the A site. An important aspect of this codon-anticodon base pairing is that only the first two nucleotides from the 5' end of the codon require Watson-Crick base pairing. The third base is termed the wobble base since Watson-Crick base pairing is not required for tRNA binding.⁹ This does not generally lead to introduction of the incorrect amino acid, however, due to codon degeneracy. Recognition of codon-anticodon pairing by the ribosome leads to positioning of the aa-tRNA 3' end in the peptidyl transferase center.¹⁰ The ribosome peptidyl transferase center catalyzes the transfer of the peptide on the P site tRNA to the A site tRNA.¹¹

After peptide transfer the deacylated tRNA and new peptidyl-tRNA translocate to the E and P sites respectively.³

Synthesis of the correct peptide also requires termination of elongation at a UAG, UGA, or UAA stop codon in the ORF. These codons do not have cognate tRNAs in most cases; the translation of UGA to selenocysteine is an example where this is not the case.¹² Eukaryotic termination is mediated by release factors eRF1 and eRF3, which are hypothesized to mimic tRNA and eEF1a respectively.¹³ eRF1 decodes the termination codon in the A site and signals the ribosome to hydrolyze the peptide-tRNA bond. eRF3 is a GTPase that binds GTP only when complexed with eRF1. GTP hydrolysis (catalyzed by the ribosome) is required for efficient peptide release, yielding a polypeptide with the correct sequence needed for further maturation into a functional protein.¹⁴ One key element that the described canonical mechanisms of translation does not take into account is the presence of cis-acting elements in the mRNA.¹⁵

Programmed -1 Ribosomal Frameshifting

mRNA cis-acting elements, such as pseudoknots, can alter translational fidelity by translational recoding.¹⁵ These elements add an additional level of regulation during protein synthesis resulting in an altered abundance of full-length protein product. Cis-acting mRNA elements can induce programmed ribosomal frameshifting, translational bypass, and codon redefinition.¹⁵ In eukaryotes one particular mode of translational recoding is predicted to be

highly abundant at approximately 10% of all messages; this recoding mechanism is programmed -1 ribosomal frameshifting (-1 PRF).¹⁶ -1 PRF was initially discovered and characterized in lentiviruses as a way to translate the gag-pol fusion protein.¹⁷ The mechanism of -1 requires specific mRNA motifs which include a heptameric “slip site” followed by a short spacer region of usually less than 12 nucleotides and a downstream secondary structure (shown in figure 2).¹⁸ The slip site sequence generally follows the format of *N NNW WWH* (IUPAC notation) where spaces separate codons of the in-coming reading frame.¹⁸ This slip site allows for movement of the A and P site tRNAs in the -1 direction since the non-wobble bases do not change.¹⁷

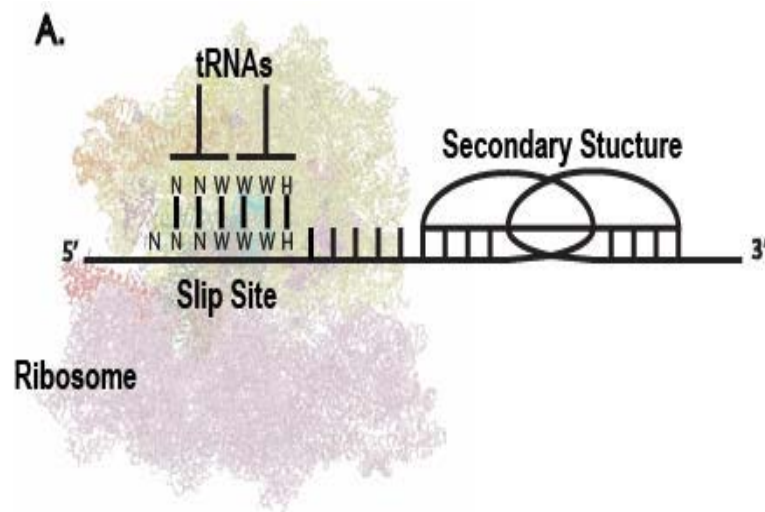


Figure 2. Structure of a typical -1 PRF signal.

The primary elements of a -1 PRF signal are the slip site and the downstream secondary structure. A short spacer of under approximately 12 nucleotides may be

The downstream secondary structure acts to impede forward movement of the ribosome, allowing for kinetic partitioning of the A and P site tRNAs

between the 0 and -1 frames.¹⁹ Stimulatory structures are generally pseudoknots, but other structures have also been shown to fulfill this role.²⁰ Three primary models for the mechanism of -1 PRF have been proposed. The first model (Pathway II in figure 3) predicts that the -1 frameshift occurs during aa-tRNA accommodation in the A site prior to peptidyl transfer. In this model the downstream stimulatory structure and binding of the aa-tRNA to codons in the A site puts tension on the mRNA. This tension is relieved by de-coupling of the A and P site tRNAs which then reposition in the -1 frame.²¹ Support for this model is provided by evidence of lower -1 PRF rates when accommodation is inhibited and greater rates of -1 PRF when peptidyl transfer is inhibited.¹⁹

The next two models occur during the translocation of tRNAs from the A and P sites to the P and E sites. The first co-translocation model (Pathway III in figure 3) suggests that incomplete translocation due to steric hindrance of the downstream stimulatory structure causes translocation of the tRNAs in the P and E sites two base pairs in the 3' direction.²¹ This results in the P and E site tRNAs positioned in the -1 frame of the slip site. Cryoelectron microscopy imaging of a -1 PRF pseudoknot blocking the tRNA exit tunnel provides some support for this mechanism.²² The second co-translocation model (Pathway I in figure 3) is similar to the first except that the incomplete translocation is predicted to occur in the previous cycle.²¹ This results in the incoming aa-tRNA to be directed to the -1 frame of the slip site. Evidence for this mechanism was shown in experiments where changes in the E site codon

sequence of the slip site affected HIV-1 -1 PRF rate.²³ Since each of these separate mechanisms of -1 PRF have supporting evidence, the mechanism of -1 PRF has been termed as a collection of kinetic partitioning events.²¹ In viruses the rate of -1 PRF can be of extreme importance for viral replication. Altering the rate of -1 PRF in HIV-1 significantly impedes replication and altered rates of -1 PRF attenuate severe acute respiratory syndrome (SARS)-associated coronavirus infectivity.^{24,25} This is due to altered stoichiometric ratios of the -1 and zero frame translation products. The first eukaryotic -1 PRF signals were discovered in the mammalian genes *Edr* and *Ma3*.^{26,27} These -1 PRF signals caused translation of a trans-frame protein from two overlapping ORFs, similar to viral -1 PRF. Contrary to these early findings, a few -1 PRF signals from yeast and the human *CCF5* -1 PRF signal do not yield a full trans-frame protein.^{28,29,30} Instead these -1 PRF signals lead to recognition of -1 frame termination codons shortly after the -1 frameshift site. Additional computational analyses of over 25 eukaryotic genomes predicted that 8-12% of genes contain at least one potential -1 PRF signal.²⁹ Over 99% of these predicted -1 PRF signals do not extend farther than 30 codons beyond the -1 frameshift site. The result of premature termination codon (PTC) recognition after a -1 PRF event has been examined with -1 PRF signals from the yeast *EST2*, *EST1*, *SCN1*, and *CDC13* mRNAs and the human *CCR5* mRNA.^{31,30} Reporter constructs containing these -1 PRF signals were shown to have a decreased mRNA steady-state abundance. Additionally, deletion of a factor required for the nonsense-

mediated decay (NMD) pathway in yeast increased endogenous mRNA abundance of EST2, EST1, SCN1, and CDC13.³¹ A potential link between NMD and -1 PRF was also shown with the CCR5 signal. Evidence for this was provided by an increase in mRNA steady-state abundance of the CCR5 -1 PRF signal when three separate NMD factors were knocked down by siRNA.³⁰

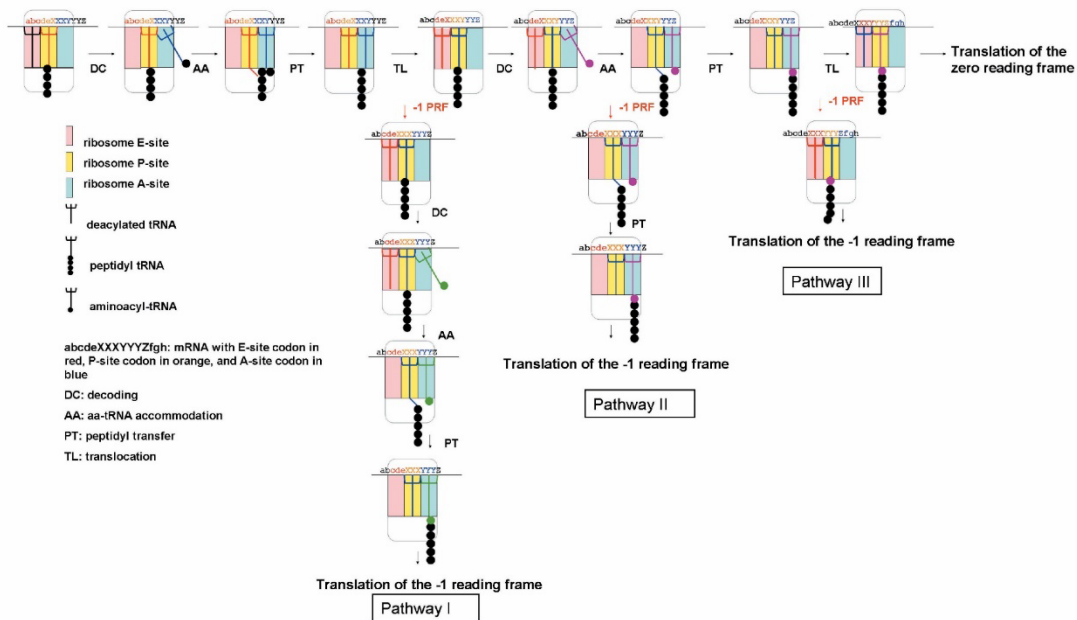


Figure 3. -1 PRF may occur through multiple kinetic partitioning pathways.

In this figure the ribosome completes two elongation cycles (top), with three alternative translation pathways that lead to a -1 frameshift shown below. In pathway I the ribosome shifts frame during the first translocation (TL) step, leading to decoding (DC) of a -1 frame codon. The second pathway to -1 frameshifting occurs during the aa-tRNA accommodation (AA) step of the second elongation cycle. A -1 frameshift may also occur due to incomplete translocation, as shown in pathway III. Figure from source 21.

Nonsense-mediated decay pathway

The NMD pathway is one of three known mRNA surveillance mechanisms. NMD is the best characterized of the three surveillance mechanisms, which include non-stop decay (NSD) and no-go decay (NGD). This pathway targets polyribosome associated mRNAs where a PTC has been recognized.³² It is hypothesized that this pathway is required to prevent synthesis of truncated proteins that have potential for negative effects on cellular function.³³ The NMD pathway is required for development of *Drosophila* and mammals, however this is not the case for yeast and *Caenorhabditis elegans*.³³ Targets of NMD include mRNA with PTCs that arise from cellular errors (like nonsense mutations or erroneous mRNA splicing) or mRNA with upstream ORFs (uORFs), translational recoding signals, or particularly long 3' untranslated regions (UTRs).^{34,35,36,37} NMD is primarily controlled by the regulator of nonsense transcript 1, 2, and 3 (UPF1, UPF2, and UPF3) proteins which are conserved among eukaryotes. UPF1 is an ATPase dependent protein with RNA binding and helicase domains that induces dissociation of the ribosome and mRNPs from the mRNA.³⁸ UPF1 also recruits exonucleases to degrade the mRNA, with the addition of endonucleolytic cleavage in metazoans.^{39,40,41} The complex of UPF2 and UPF3 associates with UPF1 through binding of UPF2 to UPF1.⁴² This interaction is important for activation of the UPF1 helicase domain.⁴³ In metazoans additional factors are required for NMD. Phosphorylation of UPF1 by SMG1 is required in all metazoans to enable recruitment of

exonucleases.⁴⁴ This phosphorylation is inhibited by SMG8 and SMG9 unless a downstream EJC is present.⁴⁵ The phosphorylated UPF1 is capable of recruiting SMG6 and a complex of SMG5-SMG7.⁴⁴ The recruited SMG6 catalyzes endonucleolytic cleavage between the EJC and the PTC, while the SMG5-SMG7 complex associate with UPF1 to promote degradation of the mRNA 5'>3' by Xrn1 and 3'>5' by the cytoplasmic exosome.^{41,46}

Two models of NMD have been proposed as mechanisms for UPF1 activation. The first is the exon junction complex (EJC) dependent model (Figure 4A), which has been characterized in mammalian cells. In this model stalling of the ribosome at a PTC stabilizes the complex of UPF1-SMG1-eRF1-eRF3 (SURF).⁴⁴ UPF1 phosphorylation by SMG1 is promoted by association with UPF2 bound to UPF3 at an exon junction complex, which needs to be at least 50-55 nucleotides downstream in mammalian cells.⁴⁷ This rule of at least 50 nucleotides does not hold true for all mammalian transcripts, suggesting that other potential cis-acting factors that induce NMD.⁴⁸ Additionally, evidence of EJC independent NMD has been provided in plants, yeast, and metazoans.^{36,37,49,50}

The *faux* 3' untranslated region (UTR) model (Figure 4B) proposes an EJC independent way for UPF1 activation. This model posits that specific mRNPs in the 3' UTR are required for normal termination, so when a premature termination codon is read this interaction no longer occurs. UPF1 is then recruited and activated due to a loss of required interactions between release

factors and 3' messenger ribonucleoproteins (mRNPs) and/or a slow rate of dissociation after peptide hydrolysis.⁵¹

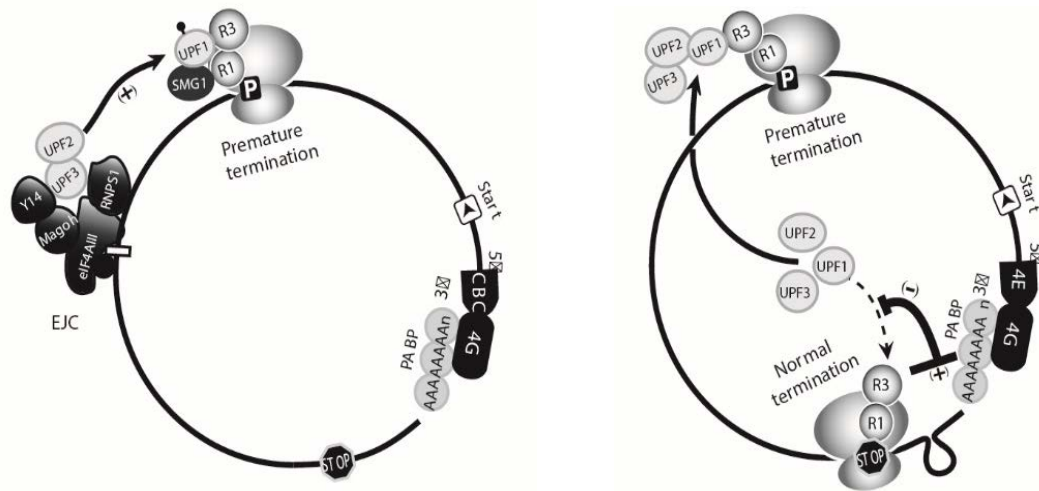


Figure 4. Two models of nonsense-mediated decay (NMD) pathway.

The exon-junction complex (EJC) model (Figure 4A) of NMD posits that the UPF2 and UPF3 factors are associated with the EJC, thus an EJC downstream of the premature termination codon (PTC) is needed for stimulation of NMD. The Faux 3' UTR model (Figure 4B) posits that factors associated with the poly (A) tail inhibit NMD if the ribosome terminates nearby. This means that the farther from the 3' end a PTC is, the more likely that mRNA will be a substrate for NMD. Figure adapted from source 33.

Based on the mechanism of NMD, it is possible that many of the potential -1 PRF signals that lead to recognition of a PTC in eukaryotes may be targets of NMD. It is important to characterize these potential -1 PRF signals in eukaryotes since the -1 PRF signals may be acting as mRNA destabilization elements. Evidence in yeast suggests that even small differences in -1 PRF

efficiency can significantly alter mRNA abundance based on exponential decreases in mRNA abundance relative to -1 PRF efficiency.³¹ This evidence suggests that altered rates of -1 PRF efficiency for a specific -1 PRF signal could have profound effects on mRNA abundance and thus protein expression. Altered protein expression due to -1 PRF could potentially disrupt cellular signaling pathways.

Potential role of -1 PRF regulation on IL2RG expression

It was previously shown that a predicted frameshift signal in the IL2RG mRNA at position 1008 from the start codon (Figure 5A) induced -1 frameshifting when tested using a bicistronic dual-luciferase reporter (Figure 5C).³⁰

Evidence of a -1 PRF signal was further supported by ribosome profiling data indicating ribosomes paused before the putative slip site (Figure 5B). This -1 PRF signal results in the recognition of a PTC, however the -1 PRF signal and PTC are located in the last exon (based on NCBI NC_000023.11 sequence). Based on the EJC criteria for NMD alone this PTC recognition would not induce NMD. In addition to the signal at 1008 is a second putative -1 PRF signal at position 354 from the start codon (Figure 6). This potential -1 PRF signal was not investigated previously, however characterization of this -1 PRF signal is important because it would lead to recognition of a PTC in exon 4 of 8. Further investigation into these -1 PRF signals will provide additional information as to whether -1 PRF plays a common role in human cells, but this research is particularly important to the study of adaptive immunity due to the function of IL2RG.

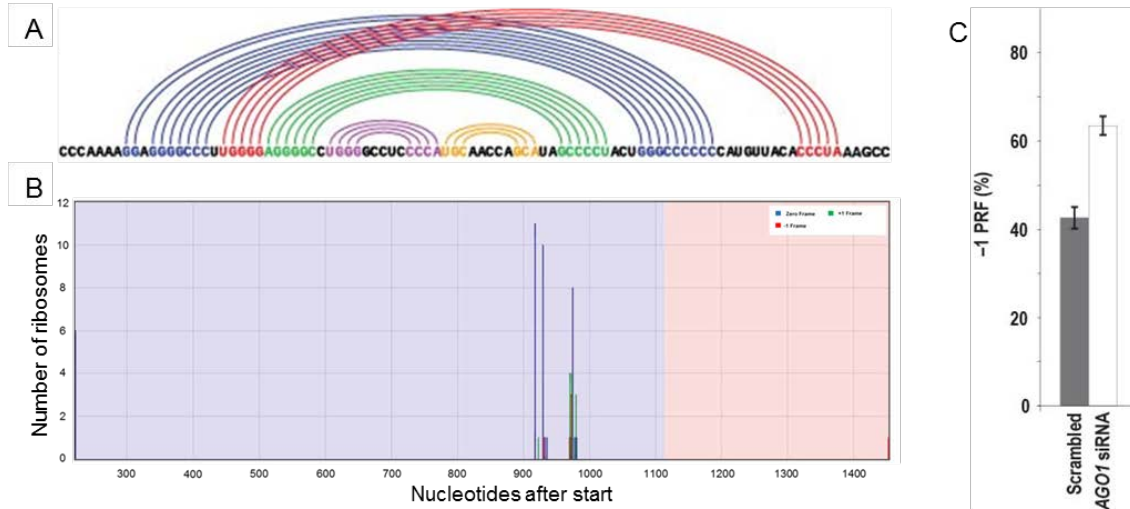


Figure 5. Predicted structure of IL2RG -1 PRF at 1008 and ribosome profiling data of IL2RG mRNA.

The Feynman diagram structure of the IL2RG -1 PRF signal at 1008 in figure 5A was predicted using the pknots folding algorithm in PRFdb. Ribosomal profiling data shows ribosomes paused within 100 nucleotides of the predicted -1 PRF signal at 1008 (Figure 5B). Unfortunately the read density for the ribosomal profiling is low, warranting possible future ribosome profiling analysis of the IL2RG mRNA to determine if a significant number of ribosomes stall at the -1 PRF signal. A test of the -1 PRF signal in the bicistronic dual-luciferase reporter pJD2034 is shown in figure 5C. This data indicates that the minimal -1 PRF signal sequence promotes efficient -1 PRF when assayed in HeLa cells. The cells were also treated with siRNA targeted against AGO1 or a scrambled control siRNA. Knockdown of AGO1 led to an increase in -1 frameshifting of the dual-luciferase reporter. Figures were adapted from source 30.

Characterized mutations in the human IL2RG gene result in various severe combined immunodeficiency (SCID) phenotypes, including the absence of T and NK cells and the presence of functionally deficient NK and B cells.^{52,53,54} Experiments to show that the IL2RG deficiency is directly responsible for SCID were performed in mice. In addition to the human phenotypes, mice also had no detectable B cell development.⁵⁵

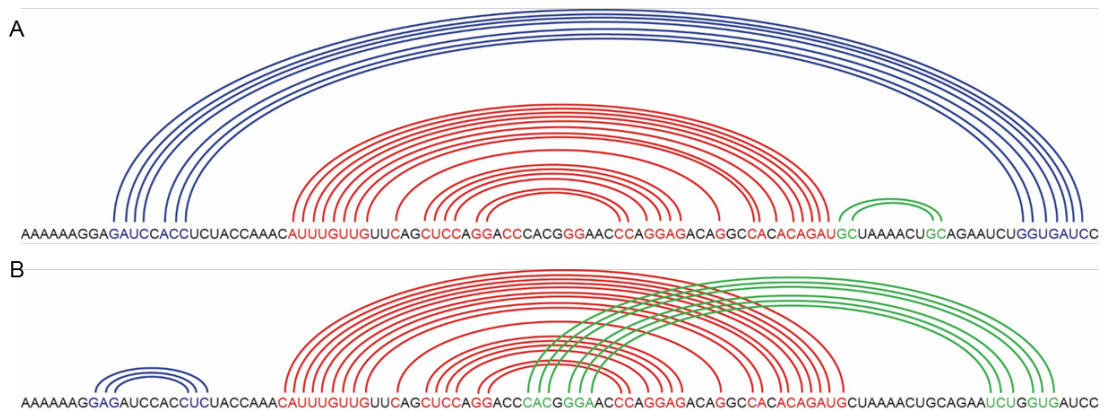


Figure 6. Predicted structures of a -1 PRF signal at position 354 of IL2RG mRNA.

The Feynman diagrams above are predicted structures of the IL2RG -1 PRF at 354 folded with the hotknots (A) and nupack (B) folding algorithms in PRFdb. The minimum free energy (MFE) of the hotknots structure (A) is -22.84 kcal/mol and the z-score is -0.33. The MFE of the nupack structure is -23.1 kcal/mol and the z score is 13.14. The pknots folding algorithm was also used to determine if there was a predicted structure, however the algorithm was unable to determine a structure.

IL2RG is a key component of the adaptive immune system because it is a component of six different cytokine receptors: IL2, 4, 7, 9, 15 and 21.⁵⁶ IL2RG

is also X-linked (thus the original disease was termed X-SCID) which means that half of the human population is particularly susceptible to disease alleles.⁵² While it is clear that mutations in IL2RG function lead to severely impaired lymphocyte replication and differentiation, overexpression of IL2RG may have a role in hyperproliferative disease. This is supported by evidence of lymphoma development in X-SCID patients undergoing gene therapy to replace functional IL2RG using lentiviral vectors.⁵⁷ Although insertional mutagenesis into oncogenic genes could explain this, gene therapy in X-SCID model mice with IL2RG led to lymphoma development in a third of the treated mice (n=15) whereas no control-vector-induced mice (n=15) developed lymphoma.⁵⁸ In addition to evidence of dysfunctional IL2RG leading to disease, there is also support for a direct correlation between IL2RG expression and lymphocyte proliferation. It was discovered in mice lacking IL2RG that gene therapy only restored T cell proliferation, however when the vector was modified to further increase IL2RG levels NK cell proliferation was also restored.⁵⁹

Although IL2RG plays a crucial role in human adaptive immunity, current knowledge on the regulation of IL2RG expression is lacking. The only known mechanism of IL2RG expression regulation is alternative splicing to yield a soluble isoform.⁶⁰ This splicing isoform lacks the transmembrane domain and has an alternative C-terminus sequence due to a shift in the open reading frame.⁶¹ The expression of JAK3, the putative kinase downstream of IL2RG signaling, also influences IL2RG expression, however the molecular basis for

this is unknown.^{62,63} Any increase in the understanding of IL2RG regulation could be invaluable to our capabilities to treat and identify diseases associated with dysregulation of IL2RG expression.

The potential -1 PRF signal discovered in the IL2RG mRNA is an important prospective form of IL2RG regulation that requires further characterization.

The presence of two predicted -1 PRF signals that would lead to recognition of PTCs means IL2RG is a possible target for NMD. -1 PRF induced NMD would lead to destabilization of the IL2RG mRNA, and thus reduce IL2RG protein abundance. The expression level of IL2RG is directly associated with the level of lymphocyte proliferation and differentiation, which in turn is important to the function of the adaptive immune system.⁵⁹ If the -1 PRF signals in the IL2RG signal are real and induce NMD, then these signals would be important to regulation of IL2RG expression and therefore function of the adaptive immune system. In order to determine if IL2RG expression is regulated by -1 PRF we aim to (1) test the -1 frameshifting efficiency of the basal -1 PRF signal sequence at 354, (2) verify the -1 PRF signal at 1008 by sequencing the trans-frame peptide, (3) analyze the effect of mutations sequenced from diseased patient tissue on the 1008 -1 PRF signal, and (4) test the basal 1008 -1 PRF signal sequence for an mRNA destabilizing effect.

Chapter 2: Results

The IL2RG -1 PRF signal at 354 promotes efficient -1 frameshifting

In addition to the previously tested -1 PRF signal at 1008, a second -1 PRF signal was predicted to be present by the PRFdb at nucleotide 354 after the start codon. The predicted structures did not appear to be particularly specific; the minimum free energy (MFE) of the structure in Figure 6A was many standard deviations higher than the mean of 100 randomized sequence MFEs, while the second (Figure 6B) was less than one standard deviation lower than the mean of 100 randomized sequence MFEs. Despite this, when tested using a bicistronic dual-luciferase reporter containing the -1 PRF signal (pJD1671), the average % -1 frameshifting in HeLa cells was 2.98% and in HEK293T cells was 1.45% (Figure 5). This sequence induces -1 frameshifting at a much higher rate than the predicted frameshift error rate of $\sim 5 \times 10^{-5}$ per codon.⁶⁴

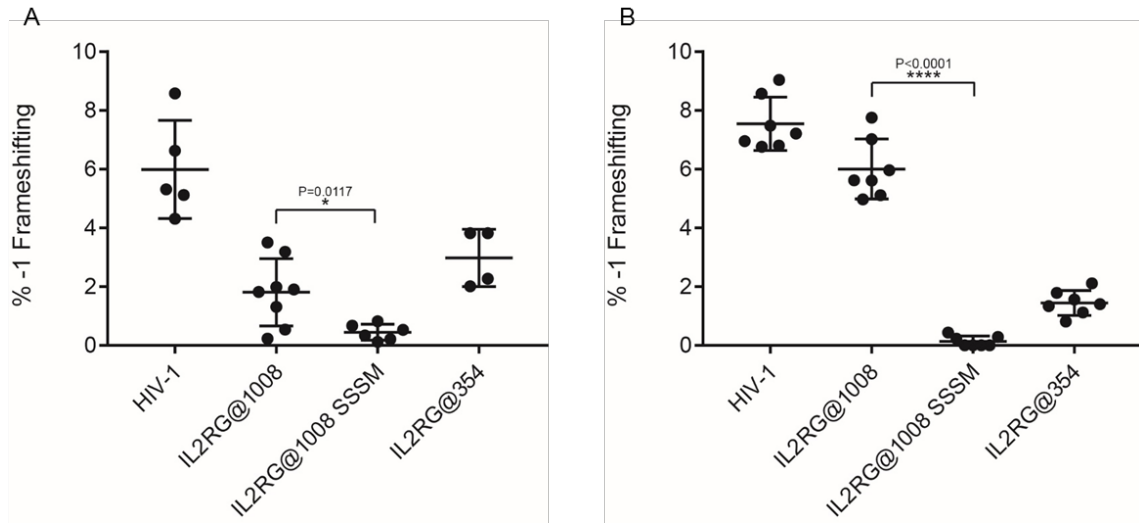


Figure 7. % -1 frameshifting of IL2RG -1 PRF signals in HeLa cells (A) and HEK293T cells (B).

Measurements of -1 frameshifting were performed with bicistronic dual-luciferase reporters. Each data point represents a single biological replicate for each test reporter assayed in triplicate. The average read-through firefly/renilla ratios for each replicate were used for calculating the % -1 frameshifting. The bars for each reporter measured represent the mean and standard deviation. A * $P < 0.05$ in HeLa cells (Figure 7A) and **** $P < 0.0001$ in HEK293T cells (Figure 7B) was calculated comparing the IL2RG -1 PRF signal at 1008 and its silent slip-site mutant (SSSM) using Welch's unequal variance's t-test. For the HEK293T cells all replicates were performed in cells passaged at least once before passaging onto 24-well plates, whereas this was not the case for all of the HeLa cell biological replicates presented.

Disrupting the slip site affects -1 frameshift efficiency of the IL2RG 1008 -1 PRF signal

Additional validation of the IL2RG -1 PRF signal at 1008 using the dual-luciferase assay was accomplished by testing mutations predicted to

specifically reduce -1 frameshifting efficiency. Silent mutations were introduced into the slip-site of the IL2RG 1008 -1 PRF containing vector pJD2034, converting the wild-type slip-site from CCCAAAA to CCCGAAG and thus inhibiting tRNA slipping. This conversion reduced the -1 frameshifting efficiency from an average of 6.01% to 0.14% in HEK293T cells (Figure 5B) and from 1.81% to 0.45% in HeLa cells (Figure 5A). Note that for the IL2RG -1 PRF signal at 1008 two A nucleotides were added directly after the slip site in order to prevent the ribosome from reading into a PTC and still synthesize the -1 frame firefly luciferase. Although these additionally nucleotides may affect the native -1 PRF signal, the dual-luciferase reporter is still useful for testing the basic function of the -1 PRF signal.

The IL2RG -1 PRF signal at 1008 induces -1 frameshifting at the slip site

One caveat of testing potential -1 PRF signals with the dual-luciferase assay is that the assay does not directly show -1 frameshifting since the output of the assay is only luciferase activity. In order to verify -1 frameshifting the trans-frame peptide (i.e. the peptide containing the shift from 0 frame coded amino acids to -1 frame encoded amino acids) needs to be purified and sequenced. This was accomplished by inserting the IL2RG -1 PRF signal shortly after the start codon of *Escherichia coli* β -galactosidase (β -GAL) and shifting the β -GAL sequence downstream of the signal to the -1 frame. In this manner the β -GAL would only be expressed if a -1 frameshift event occurred, thus allowing for affinity purification of β -GAL in order to obtain the trans-frame peptide. Once again, two nucleotides were required after the slip site in

order for the -1 frame β -GAL to be synthesized without reading into a PTC. As mentioned previously, this may alter the wild-type function of the -1 PRF signal, however the reporter still performs the purpose of determining if the -1 PRF signal causes -1 frameshifting at the slip site. β -GAL was chosen as an affinity tag because it allows for screening of the protein throughout the purification process by assaying for β -GAL hydrolysis of o-nitrophenyl- β -galactopyranoside (ONPG).

```

1      MTSRILEHFSQEDAPDEMCKYIKSFERVVLKNEQMSTPKIGGALGEGPGAS
52     PCNQHSPYWAPPCYTLKPE TGTDPVVLQRRDWENPGVTQLNRLAAHPPF
101    ASWRNSEEARTDRPSQQLRSLNGEWRFAWFPAPEAVPE SWLECDLPE AD
150    TVVVPSNWQM HGYDAPIYTNVYPTVNPFFVPTENPTGCYSLTFNVD E S
200    WLQEGQTRIIDGVNSAFHLWCNGRWVGYGQDSRLPSE FDLSAFLRA GEN
250    RLAVMVLRWSDGSYLEDQDMWRMSGIFRDVSL LHKPTTQISDFHVATR FN
300    DDFSRAVLEAEVQMC GELRDYLRVTVSLWQGE TQVASGTAPFGGEIIDE R
350    GGYADRVTLRLN VENPKLWSAEIPNLYRAVVELHTADGTLIE AEACDVGF R
401    EVRIENGLLLLNGKPLLIRGVNRHEHHPLHGQVMDEQTMVQDILLMKQNNF
452    NAVRCSHYPNHPLWYTLCDRYGLYVVDEANIETHGMVPMNRLTDDPRWLP
502    AMSERVTRMVQRDRNHPSVIIWSLGNESGHGANHDALYRWIKSVDPSPRV
552    QYE GGGADTTATDIICPMYARVDE DQPFPAVPKWSIKKWLSPGETRPLIL
603    CEYAHAMGNSLGGFAKYWQAFRQYPR LQGGFVWDWVDQSLIKYDENG NP
652    WSAYGGDFGDTPNDRQFCMNGLVFADRTPHPALTEAKHQQQFFQFRLSG
701    QTIEVTSEYLF RHSDNELLHWMVALD GKPLASGEVPLDVAPQGKQLIELPE
752    LPQESAGQLWLTVRVVQP NATAWSE AGHISAWQQWR LAENLSVTLPAAS
802    HAIPHLTTSEMDFCIE LGNKRWQFN RQSGFLSQMWIGDKKQLLTPLRDQF
852    TRAPLDNDIGVSE ATRIDPNAWVERWKAAGHYQAE AALLQCTADTLADAV
902    LITTAHAWQHGGKTLFISRKTYRIDGSGQMAITVDVEVASDTPHPARIGLN
953    CQLAQVAE RVNWLGLGPQ ENYPDLRTAACFDRWDLPLSDMYTPYVFPSE
1002   NGLRCGTRELNYGPHQWRGDFQFNISRYSQQQLMET TSHRHLHLHAEEGTW
1051   LNIDGFHMGIGGDDSWSPSVA EFQLSAGRYHYQLVWCQK

```

Figure 8. LC-MS/MS sequence coverage of IL2RG@1008:: β -GAL.

Sequenced peptides highlighted in green cover 22.3% of the fusion protein. Black amino acids are β -GAL sequence. The grey amino acids are a spacer taken from Renilla luciferase. The blue amino acids are zero-frame IL2RG and the red amino acids are -1 frame IL2RG.

Once purification of the trans-frame peptide from yeast was accomplished the protein sequence was determined by liquid chromatography-tandem mass spectrometry (LC-MS/MS). The mass spectrometry sequencing covered

22.3% of the total IL2RG:: β -GAL fusion protein (Figure 6). A total of 17 peptides were discovered above a cross-correlation value of 2.10 or an ion score above 36 and contained the predicted trans-frame peptide (Figure 7). The spectrum with the highest Sequest cross-correlation (4.68) and Mascot ion score (44) is shown in figure 8 and highlighted in Figure 7. These values indicate that there is no significant difference ($p < 0.5$) between the observed and predicted peptide m/z values. y and/or b ions for all fragmentation sites were detected except those predicted for the first four and the last two amino acids.

Start-End	Observed	Mr (expt)	Mr (calc)	ppm	Miss	Sequest xcorr	Mascot ion score	Sequence
28-70	945.8660	4724.2938	4724.2461	1	2	4.55	38	E.RVLKNEQMSTPKIGGALGEGPGASPCNQHSPYWAPPCYTLKPE.T + 2 Deamidated (NQ)
28-70	949.0630	4740.2789	4740.2410	5	2	3.66	13	E.RVLKNEQMSTPKIGGALGEGPGASPCNQHSPYWAPPCYTLKPE.T + 2 Deamidated (NQ) ; Oxidation (M)
28-70	949.2637	4741.2823	4741.2251	1	2	3.89	26	E.RVLKNEQMSTPKIGGALGEGPGASPCNQHSPYWAPPCYTLKPE.T + 3 Deamidated (NQ) ; Oxidation (M)
34-46	644.8319	1287.6493	1287.6493	1	0	2.45	27	E.QMSTPKIGGALGE.G
34-70	996.7114	3982.8166	3982.8441	1	1	4.27	41	E.QMSTPKIGGALGEGPGASPCNQHSPYWAPPCYTLKPE.T
34-70	996.7193	3982.8480	3982.8441	2	1	4.42	21	E.QMSTPKIGGALGEGPGASPCNQHSPYWAPPCYTLKPE.T
34-70	996.9691	3983.8474	3983.8281	2	1	2.62	12	E.QMSTPKIGGALGEGPGASPCNQHSPYWAPPCYTLKPE.T + Deamidated (NQ)
34-70	997.2156	3984.8332	3984.8121	2	1	3.84	20	E.QMSTPKIGGALGEGPGASPCNQHSPYWAPPCYTLKPE.T + 2 Deamidated (NQ)
34-70	997.2188	3984.8459	3984.8121	1	1	4.11	41	E.QMSTPKIGGALGEGPGASPCNQHSPYWAPPCYTLKPE.T + 2 Deamidated (NQ)
34-70	997.2194	3984.8483	3984.8121	1	1	3.53	24	E.QMSTPKIGGALGEGPGASPCNQHSPYWAPPCYTLKPE.T + 2 Deamidated (NQ)
34-70	1000.7144	3998.8286	3998.8390	3	1	2.67	15	E.QMSTPKIGGALGEGPGASPCNQHSPYWAPPCYTLKPE.T + Oxidation (M)
34-70	1000.7158	3998.8340	3998.8390	10	1	3.24	15	E.QMSTPKIGGALGEGPGASPCNQHSPYWAPPCYTLKPE.T + Oxidation (M)
34-70	1000.7176	3998.8413	3998.8390	1	1	4.68	44	E.QMSTPKIGGALGEGPGASPCNQHSPYWAPPCYTLKPE.T + Oxidation (M)
34-70	1333.9559	3998.8460	3998.8390	3	1	3.30	15	E.QMSTPKIGGALGEGPGASPCNQHSPYWAPPCYTLKPE.T + Oxidation (M)
34-70	1000.9694	3999.8483	3999.8230	1	1	3.36	16	E.QMSTPKIGGALGEGPGASPCNQHSPYWAPPCYTLKPE.T + Deamidated (NQ) ; Oxidation (M)
34-70	1001.2160	4000.8349	4000.8070	4	1	4.10	13	E.QMSTPKIGGALGEGPGASPCNQHSPYWAPPCYTLKPE.T + 2 Deamidated (NQ) ; Oxidation (M)
34-70	1334.9552	4001.8438	4001.7910	1	1	3.67	21	E.QMSTPKIGGALGEGPGASPCNQHSPYWAPPCYTLKPE.T + 3 Deamidated (NQ) ; Oxidation (M)

Figure 9. Table of all trans-frame peptides sequenced by LC-MS/MS.

The spectrum for the peptide highlighted in yellow was chosen as a representative sample since it had the highest cross-correlation at 4.68 compared with the theoretical mass spectrum of the peptide as determined by the Sequest HT (v1.17) program.

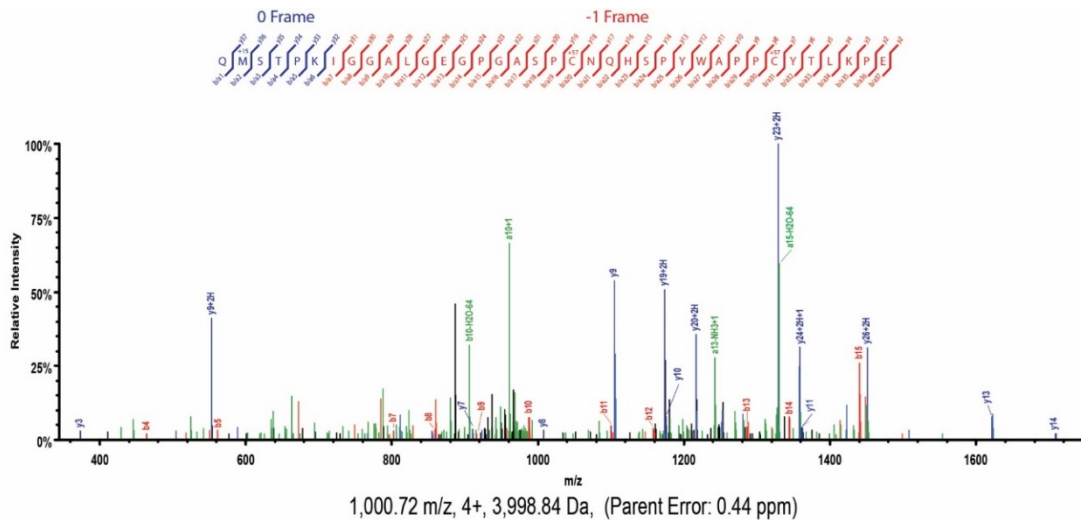


Figure 10. Mass spectrum of the IL2RG -1 PRF at 1008 trans-frame peptide.

Mass spectrum was obtained by liquid chromatography-tandem mass spectrometry (LC-MS/MS). Above the spectrum is the peptide sequence with fragmentation sites of b/a and y ions shown. The sequence in blue is zero frame peptide and the sequence in red is -1 frame peptide. The number above the methionine is the approximate mass addition in Da due to oxidation and the number above the cysteines is the approximate mass addition in Da due to carbamidomethylation. The m/z, charge, and size of the parent peptide is shown below the spectrum.

Mutations in the IL2RG 1008 -1 PRF signal are present in cancer patients

The sequence of the trans-frame peptide induced by the IL2RG -1 PRF signal establishes that the signal is real, however the potential role of this -1 PRF signal remains to be determined. In order to gain some understanding of the -1 PRF signals potential role in cells, publicly available IL2RG patient gene sequences were mined for mutations within the -1 PRF signal. The goal of mining for mutations was to discover potential disease phenotypes, which would then indicate potential roles for the -1 PRF signal in cells. The results of

mining the Ensembl genome browser for mutations are shown in figure 9. Based on this search the only known mutations in the IL2RG -1 PRF signal at 1008 are associated with either no alternative phenotype or cancer.

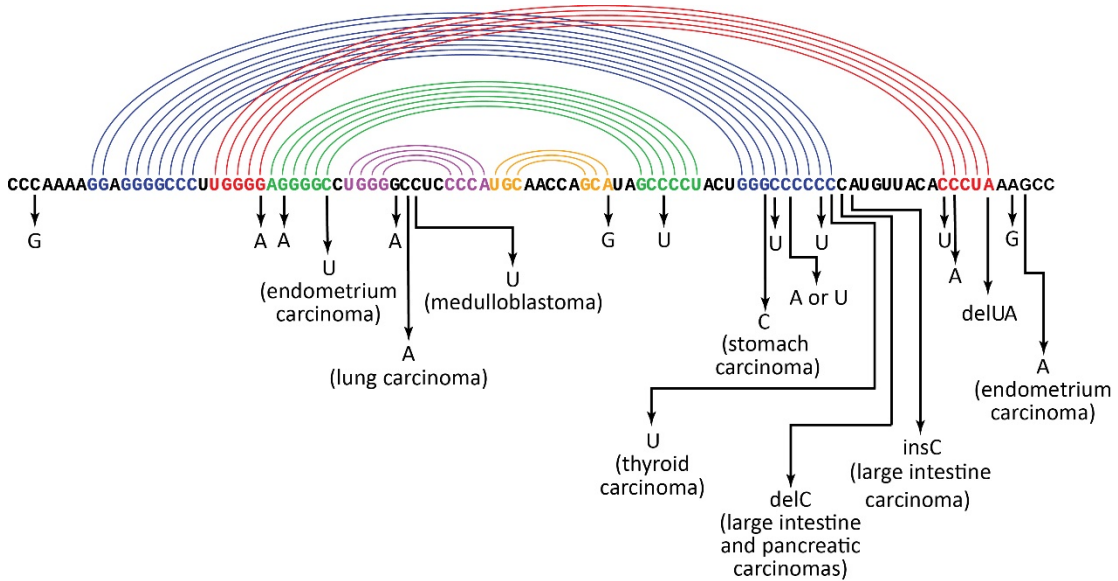


Figure 11. Patient mutations found in the IL2RG -1 PRF signal at 1008.

Mutations were found using the Ensembl database and mapped to the Feynman diagram of base pair interactions predicted using the pknots algorithm. All mutations that were sequenced from cancer tissue have the cancer type listed below.

Cancer associated mutations reduced -1 PRF efficiency

Five of the cancer associated single nucleotide polymorphisms (SNPs) in the IL2RG -1 PRF signal at 1008 were cloned into the dual-luciferase reporter vector and tested for effects on -1 PRF efficiency. The SNPs tested are shown in table 1.

Reference Number	Ribonucleotide Change	Amino Acid Change	Plasmid Number
COSM1558340	C1043→A	A348→D	pJD1539
COSM1124594	C1036→U	P346→S	pJD1540
COSM3372325	C1081→U	P361→S	pJD1541
COSM4110798	G1075→C	A359→P	pJD1542
COSM1124593	G1098→A	K366→K	pJD1543

Table 1. Cancer associated SNPs tested in dual luciferase reporter.

The results of the effect of each SNP on -1 PRF efficiency are shown in figure 12. There was no significant difference between the wild-type (WT) IL2RG -1 PRF signal at 1008 and the silent slip-site mutant (SSSM), or WT and any of this SNPs. However, there is a visible trend of reduced -1 PRF efficiency when the SNP is introduced and previously it was shown that SSSM significantly differs from WT. This suggests that more replicates need to be performed in order to make any arguments about the data.

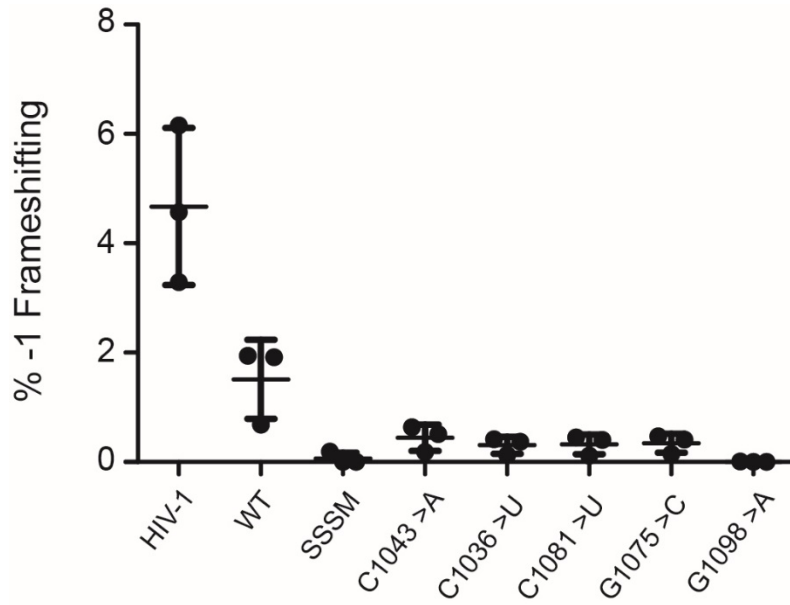


Figure 12. % -1 frameshifting of IL2RG -1 PRF signal at 1008 with cancer associated SNPs.

Measurements of -1 frameshifting were performed with bicistronic dual-luciferase reporters. HIV-1 was used as a positive -1 PRF control. Each data point represents a single biological replicate for each test reporter assayed in triplicate. The average read-through firefly/renilla ratios for each replicate were used for calculating the % -1 frameshifting. The bars for each reporter measured represent the mean and standard deviation. WT refers to the wild-type IL2RG -1 PRF signal at 1008 reporter (pJD2034) and SSSM refers to the silent slip-site mutant reporter (pJD1544). The five SNP containing reporters are labeled by the ribonucleotide change.

Chapter 3: Discussion

In addition to the IL2RG -1 PRF signal starting at 1008 it appears that a second predicted -1 PRF signal starting at nucleotide 354 from the start codon can induce efficient -1 frameshifting. This putative -1 PRF signal needs further validation before being defined as a -1 PRF signal. Further investigation on this 354 -1 PRF signal is important because of a -1 frame PTC just downstream of the slip site in exon 4. This -1 frame PTC would be predicted to induce efficient NMD based on the EJC model of NMD because it is 94 bases upstream of the next splice site (based on NCBI NC_000023.11 sequence).⁴⁷ In this way the -1 PRF signal could act as an mRNA destabilizing element.

The IL2RG predicted -1 PRF signal at 1008 can now be defined as a canonical -1 PRF signal. This was verified by the LC-MS/MS sequencing of a trans-frame peptide resulting from a -1 frameshift at the predicted slip site. The mass spectrometry data is supported by the fact that introducing silent mutations into the slip site essentially ablates -1 PRF (Figure 5). Further work will need to be performed with this -1 PRF signal in order to determine its relevance in endogenous IL2RG mRNA. However, efficient -1 PRF induced by the basal signal sequence does prove that this sequence has the potential to induce efficient -1 PRF in endogenous IL2RG mRNA.

Interestingly, these -1 PRF efficiencies measured by the dual-luciferase assay varied depending on the cell type in which it is assayed. In HEK293T cells the -1 frameshifting ranged from 4.97-7.75% while in HeLa cells this efficiency

ranged from 0.23-3.50%. Additionally the HeLa cell -1 PRF efficiencies reported here are significantly lower than previous data.³⁰ These differences in -1 PRF efficiency exemplify the importance of the cellular environment on -1 PRF rates. One hypothesis that could explain this is the presence of trans-acting factors. Future investigation into this possibility is supported by research showing an interaction between miR-1224 and CCR5.³⁰

Unlike the -1 PRF signal at 354, the 1008 -1 PRF signal does not lead to recognition of a -1 frame PTC with a downstream EJC, thus indicating that the -1 PRF signal may not induce NMD. This prediction is supported by recent data suggesting that in humans a downstream EJC is required for efficient NMD.⁶⁵ However, this does not disprove the potential for the IL2RG -1 PRF at 1008 to act as a destabilization element. This may be possible by induction of NMD based on the *faux* 3' UTR model, or alternatively induction of the NGD pathway due to stalling of the ribosome at the -1 PRF signal's secondary structure.⁶⁶ This requires further investigation by initial testing of the basal -1 PRF signal sequence on mRNA stability.

A search for disease associated mutations in the validated IL2RG 1008 -1 PRF signal was performed to determine a potential physiological role, thus providing future research goals. Only the presence of mutations sequenced from patient cancer tissue or SNPs with no known phenotype could be found in the -1 PRF signals. The mutations sequenced from patient cancer tissue could be due to the mutagenic environment of the cancer tissue itself or benign SNPs, however these mutations may also have an oncogenic

properties which requires further investigation. The best way to provide evidence that the SNPs can be oncogenic is by introducing the SNPs via CRISPR-Cas9 into a lymphocyte cell line. Unfortunately these experiments are not tractable.

Another, less direct, route to determine if the mutations have transformative potential is to determine if the mutations alter -1 PRF efficiency of the 1008 signal. The five cancer associated SNPs that were tested all show a visible, but not determined significant, decrease in -1 PRF efficiency relative to the wild-type IL2RG -1 PRF signal. The reduction in -1 PRF efficiency observed could affect expression of IL2RG by either altering the stability of the message (a result that still requires testing for the 1008 -1 PRF signal) or by altering the stoichiometry between the full-length IL2RG and a dysfunctional truncated IL2RG. If mutations in the -1 PRF signal reduced -1 PRF efficiency by weakening the stimulatory secondary structure, they could potentially either increase mRNA stability based on previous work showing that mRNA stability exponentially decreases as a function of -1 PRF efficiency.³¹

Alternatively, a decrease in -1 PRF efficiency could lead to an increase in the abundance of full-length IL2RG. If the truncated IL2RG protein is dysfunctional, then an increase in the amount of full length IL2RG would phenocopy increased IL2RG expression. Previous research has shown a positive correlation between IL2RG expression and lymphocyte proliferation, which may be a risk factor for lymphoma development.⁵⁹ Evidence for this has been shown in X-SCID patients and mouse models in which expression of

functional IL2RG led to lymphoma in a subset of patients/mice.^{57,58} In addition to lymphoma it is also possible for the increased expression of IL2RG to lead to cancer in other tissue types through increased inflammation in a model similar to Hepatitis C Virus.⁶⁷ This is supported by the fact that IL2RG is a component of pro-inflammatory pathways via interaction with IL7, IL9, IL15, and IL21.^{68,69,70,71} The work described herein provides a framework for designing future studies to elucidate the role of IL2RG -1 PRF in normal physiological responses and pathological conditions.

Chapter 4: Materials and methods

Plasmid construction

Plasmids with pJD numbers 1980, 1979, 2001, 1666, 1665, 1544, 1533-1536, and 1667-1676 were created using the In-Fusion HD Cloning kit (Clontech). gBlocks from IDT were used as inserts for plasmids 1980, 1979, 2001, 1666, 1665, 1533, and 1534 while plasmids 1544, 1667-1676, 1535, and 1536 were created using over-lapping 90 bp oligonucleotides. gBlocks and overlapping oligonucleotides were designed to have a T_m of $>50^\circ\text{C}$ at all overlapping sites and overlap by >15 bp with sites to be joined to. Linear 1980, 1979, 1666, 1665, and 1533 were generated by digesting with KpnI and XhoI FastDigest enzymes (Thermo Fisher). Linear 2001, 1667-1676, and 1544 were digested using BamHI and Sall FastDigest enzymes. Linear 1534 was created by digestion with Accl and SpeI FastDigest enzymes. Linear 1535 and 1536 were created by digestion with HindIII and Sall FastDigest enzymes. All FastDigest digestions were performed according to the manufacturer protocols, however the digestion times ranged from 15 minutes to 3 hours. Products from the In-Fusion HD cloning reaction were transformed into the Stellar competent cells provided with the In-Fusion HD kit according to manufacturer instructions. Transformed cells were plated on LB agar with ampicillin (50 $\mu\text{g}/\text{mL}$) for selection. Plasmids were purified from transformed cells using the GeneJET Plasmid Miniprep Kit (Thermo Fisher) according to manufacturer instructions. Verification of successful clones was done by analysis of sequencing performed by GENEWIZ.

Plasmids with pJD numbers 1538-1543 and 2094-2099 were generated by oligonucleotide-directed mutagenesis using the QuikChange Lightning Site-Directed Mutagenesis Kit (Agilent). Oligonucleotides for mutagenesis were designed to end in at least one G or C, have >15 bases on either side of the nucleotide to be mutated, and a GC content of >40%. These oligonucleotides are listed in Appendix A. Reactions and transformations were performed according to the manufacturer instructions, with the alternative of using the In-Fusion HD Stellar competent cells for transformation. The plasmid used for mutagenesis to make 2094-2099 was pJD1535 and for 1538-1543 is was pJD2034. Transformed cells were plated on LB agar with ampicillin (50 µg/mL) for selection. Plasmids were purified from transformed *E. coli* using the GeneJET Plasmid Miniprep Kit. Verification of successful clones was done by analysis of sequencing performed by GENEWIZ.

Plasmids with pJD numbers 2075-2081 were cloned by conventional digestion and ligation methods. In order to remove the SV40 promoter from pJD1538-pJD1544 plasmids were digested with FastDigest enzymes KpnI and PstI for 1.5 hours. Digested plasmid was run on a 0.8% agarose gel then excised and purified using the GeneJET Gel Extraction Kit (Thermo Fisher) according to the manufacturer protocol. The CMV promoter was removed from pJD2044 using KpnI and PstI as well and purified from agarose gel using the GeneJET Gel Extraction Kit. The CMV promoter insert was ligated into each of the digested plasmids with the Quick Ligation Kit (NEB). The reaction mix consisted of 50 ng of digested plasmid, 19.55 ng of the CMV

insert, 10 μ L of 2X Quick Ligase Reaction Buffer, and enough nuclease-free water to reach a final volume of 20 μ L. The mixture was left at room temperature for 15 minutes then 5 μ L of the mixture was using for transforming into Stellar competent cells according to the manufacturer's protocol. Transformed cells were plated on LB agar with ampicillin (50 μ g/mL) for selection. Successful clones were screened for by diagnostic digestions with KpnI and PstI FastDigest enzymes to verify insertion of the CMV promoter by size. A second diagnostic digestion was performed with NdeI FastDigest enzyme, which was a restriction site unique to the CMV promoter to further verify insertions.

The plasmid pJD2106 was created by Jordan Aoyama in order to generate a new version of the rabbit β -globin mRNA stability reporter. The backbone of this plasmid (pTRE3G-BI Clontech) was initially modified by replacement of the multiple cloning sites (MCSs) flanking the bi-directional promoter of the plasmid with new MCSs. The HindIII site in the promoter region of pTRE3G-BI was deleted using the QuikChange Lightning Site-Directed Mutagenesis Kit (Agilent) and oligonucleotides 48 and 49 (Appendix A). MCS1 was digested out of the plasmid using EcoRV and Sall. A new MCS was cloned into this linear construct using the In-Fusion HD Cloning kit (Clontech) and the overlapping oligonucleotides 50 and 51 (Appendix A). MCS2 was digested out of the plasmid using XbaI and EcoRI. A new MCS was cloned into this linear construct using the In-Fusion HD Cloning kit (Clontech) and the overlapping oligonucleotides 52 and 53 (Appendix A). The rabbit β -globin

gene in pJD976 was digested out using *SpeI* and *BglIII*, gel purified and ligated (Quick Ligation kit NEB) into the modified pTRE3G-BI linearized with *SpeI* and *BglIII*. A gblock containing GFP was inserted using the In-Fusion HD Cloning kit (Clontech) into the modified pTRE3G-BI linearized with *PacI* and *SwaI*. Next this modified pTRE3G-BI with β -globin and GFP was digested with *PciI* followed by phosphatase treatment in order to prepare it for addition of blunt end adapters that would delete the *SspI* site upon addition of a hygromycin resistance cassette (oligonucleotides 54 and 55 in Appendix A). The 5' phosphorylated adapters were inserted into this linear construct by ligation using the Quick Ligation kit (NEB). Finally, a hygromycin resistance insert from p*Silencer* 3.1-H1 hygro was excised by digestion with *SspI*, then ligated into the linear modified pTRE3G-BI with blunt end adapters. The result of this ligation was pJD2106.

In order to create pJD2113-2121 the plasmids pJD1035, 1535-1536, and 2094-2099 were digested using *MlsI* and *SpeI* and the β -globin containing insert was gel purified. This insert was ligated into pJD2106 linearized with *MlsI* and *SpeI* using the Quick Ligation kit (NEB). The pJD1035 insert was used to create pJD2113. The pJD1535 and 1536 inserts were used to create pJD2114 and 2115 respectively. pJD2094-2099 inserts were used to create pJD2116-2121 respectively. Insertions were verified by sequencing (GENEWIZ)

The pJD2044 dual-luciferase reporter with a CMV promoter was created by Joseph Briggs as follows. 1ng of the plasmid pCDNA3.1(+) (Invitrogen) was

used as template for PCR amplification of the CMV promoter/enhancer using the primers listed as 57 and 58 in Appendix A (each at 0.2 μ M/reaction). The forward primer contains a KpnI restriction enzyme digestion site whereas the reverse primer contains a PstI site to allow for subsequent cloning into similarly digested plasmids. PCR was done using DreamTaq Hot Start PCR Mastermix (ThermoFisher) using the following cycling parameters: Step1= 95C for 2min; Step 2= 95C for 30sec, 60C for 30sec, 72C for 1min and repeat Step 2, 24 times. PCR products were separated on a 1% agarose gel, visualized with ethidium bromide under UV light and gel purified using a GeneJet agarose gel purification kit (ThermoFisher). Gel purified PCR products were subsequently digested using the restriction enzymes KpnI and PstI followed by column purification using a Nucleospin Gel and PCR Cleanup kit (Machery-Nagel). The product was then ligated into a similarly digested and gel purified pJD175f plasmid backbone resulting in the plasmid pJD2044. Insertion of the CMV promoter/enhancer was verified by restriction digestion and the identity confirmed by DNA sequencing.

Yeast transformations

Alkali-cation yeast transformation was used to create strains 1716, 1717, 1719-1725, and 1752 with the following protocol specifics. Yeast were initially grown overnight in 5 mL cultures of YPAD medium. 200-600 μ L of cell culture was then centrifuged down using a microcentrifuge at 4000xg for 1 min followed by a wash with 200 μ L of 0.1 M LiOAc/TE. Yeast were resuspended in 100 μ L of 0.1 M LiOAc/TE. 10-20 μ L of salmon sperm ssDNA (denatured at

80°C for 5 min) and 500-2000 ng of plasmid DNA were then added to the cells and vortexed lightly. 600 μ L of a 0.1 M LiOAc/TE solution with 50% PEG 3350 was then added to the cells and mixed in by light vortexing. The cells were given 45 min to an hour to incubate at 30°C before a 7-10 min heat shock at 42°C. After heat shock the yeast were spun down by centrifugation at 4000xg for 1 min then washed with 1 mL of water. Cells were resuspended in 200 μ L of water and plated on selective media (-Trp for strains 1716, 1717, and 1752; -Ura for all other strains made). Transformed yeast were allowed to grow for 1-3 days before a single colony is picked to become the stock strain. Yeast strains 1716, 1717, and 1752 successful transformations were verified further by β -galactosidase assay, and strains 1716 and 1717 were additionally verified by plasmid rescue.

β -galactosidase (β -GAL) assay

In order to verify transformations of yeast with any of the pTI25-based constructs and to monitor protein abundance during purification the β -GAL activity was assayed by colorimetric quantification of ONPG hydrolysis. Intact yeast were assayed for β -GAL activity by initially pelleting down 50 μ L to 2 mL of either cell culture or previously concentrated cells and removing the supernatant. Cells were then resuspended in 450 μ L of cold Z buffer (60 mM Na_2HPO_4 , 40 mM NaH_2PO_4 , 10 mM KCl, 1 mM MgSO_4 , and 50 mM β -mercaptoethanol). 100 μ L of chloroform and 1 μ L of 10% sodium dodecyl sulfate (SDS) were then added to lyse the cells. For assays performed with cell lysate or any downstream steps of β -GAL purification 5-50 μ L of the

sample was diluted to 500 μL with Z buffer with no addition of chloroform or SDS. Once the samples (both intact yeast and post-lysis step sample) are in Z buffer they were vortexed vigorously and left to incubate at room temperature for >5 min. Next 100 μL of ONPG (4 mg/mL in PBS) was added and the reaction time was measured. As a negative control, samples were prepared with 100 μL of PBS instead of ONPG. The reaction was quenched with 1 M Na_2CO_3 after the solution turned visibly yellow. The optical density of the solution was measured at 420 nm using the negative control as a blank. In order to determine the approximate amount of β -GAL in solution the OD420/time was plotted against a standard curve for OD420/time as a function of ng β -GAL in the reaction. This standard curve was generated using *Escherichia coli* β -GAL (Sigma-Aldrich) at 10, 5, 1, 0.1, and 0.01 ng per reaction using the post-lysis β -GAL assay protocol with each concentration of β -GAL assayed in triplicate with separate aliquots of dilute protein.

Mammalian cell culture

All mammalian cell lines were cultured in a water-jacketed CO_2 incubator at 37°C and 5% CO_2 . HeLa (ATCC LOT#63226283) and HEK293T (ATCC LOT#62729596) cells were grown in Dulbecco's Modified Eagle's Medium (DMEM) with 4.5 g/L glucose, L-glutamine, and sodium pyruvate (Corning) and supplemented with USDA Approved Origin Fetal Bovine Serum (Seradigm CAT#1300-050) at 10% and penicillin-streptomycin at 100 units/mL (Gibco). This media is referred to as DMEM++. HeLa Tet-Off (Clontech) were cultured DMEM++ with the addition of G418 at 200 $\mu\text{g}/\text{mL}$.

Cells were grown on cell-culture treated T75 flasks, 6 well plates, 12 well plates, or 24 well plates. The volume of media used for each culture container was 10 mL, 3 mL/well, 1 mL/well, and 0.5 mL/well respectively.

Cells were maintained by passaging at high confluency. To passage cells aliquots of trypsin, PBS, and the appropriate media were incubated in a 37°C water bath for >5 min. Old media from the cells was removed by aspiration then cells were washed with warm PBS to remove any remaining media.

Cells were then treated with 5-6 mL of warm trypsin and incubated at 37°C for 5-10 min. Trypsin inactivation was accomplished by the addition of an equal volume of culture medium. Cells were pelleted by centrifugation at 150xg, 23°C for 5 min. The supernatant was aspirated and cells were resuspended in 2-4 mL of culture media, depending on the size of the cell pellet. Cell counts were performed using a TC20 Automated Cell Counter (Bio-Rad) following manufacturer instructions. Cell dilutions were performed as necessary in culture media to achieve the correct concentration of cells to be plated. When passaging cells into a new T75 flask $>1 \times 10^5$ cells were grown in 10 mL of culture media.

Mammalian cell transfections

HeLa, HEK293T, and HeLa Tet-Off cells were plated in 24 well plates at 5×10^4 - 8×10^4 cells per well, in a 12 well plate at 8×10^4 cells per well, or in a 6 well plate at 1.5×10^5 cells per well. Cells were transfected at either 24 hours or after reaching >70% confluency. All plasmids used for cell transfection were purified using the ZymoPURE Plasmid Midiprep Kit (Zymo Research) to

obtain large amounts of endotoxin-free plasmid DNA. Cell transfections were performed with FuGene HD transfection reagent (Promega) according to the manufacturer's directions. For 24 well plates transfection complexes were prepared by diluting 550 ng of plasmid stock to 23.3 μ L with non-supplemented DMEM then mixing with 1.7 μ L of FuGene HD transfection reagent. For 12 well plates transfection complexes were prepared by diluting 1 μ g of plasmid stock to 37 μ L with non-supplemented DMEM, followed by addition of 2.95 μ L of FuGene HD reagent. Transfection complexes were mixed by vortexing, quickly spun down using a microcentrifuge, and then incubated for 15 minutes at room temperature. The entire complex volume was added to the cells and mixed with the media by rocking back and forth gently.

-1 PRF dual-luciferase assays

All assays were performed with lysate from transfected HeLa, HEK293T, or HeLa Tet-Off cells. All assays were performed using the Promega Dual-Luciferase Reporter Assay System with specifics as follows. Cells were lysed between 24 and 48 hours post-transfection. Prior to lysis cells were washed twice with 500 μ L of PBS. Lysis was performed by addition of 100-120 μ L 1x passive lysis buffer per well for 24 well plates or 220 μ L for 12 well plates followed by vigorous rocking for 5 minutes. Assays were performed using 30 μ L of lysate per well in triplicate using a GloMax Multi Detection System luminometer (Promega). 50 μ L of each reagent was injected per well with a 10 sec integration and 2 sec pauses between each read. A minimum of three

biological replicates or enough replicates to achieve a normal distribution were performed per sample as previously described.⁷² All reads were corrected for background luminescence prior to normalization by subtraction of the relative signal intensity measured for each replicates no plasmid control. Any corrected reads that were negative (this was only the case for the firefly reads of the 1008 IL2RG -1 PRF silent slip-site mutant) were changed to zero after normalization for presentation. Differences between test groups were determined significant using an unpaired Welch's unequal variances t-test.

Production and purification of IL2RG -1 PRF:: β -GAL fusion protein from yeast

The yeast strain yJD1717 was created by transformation of yJD1370 with pJD1980. Six 5 mL culture tubes containing defined medium lacking tryptophan (-Trp) were inoculated with yJD1717 and grown overnight in a 30°C shaker incubator at 250 rpm. The next day each single culture tube was used to inoculate a single 2 L baffled flask containing 500 mL of the -Trp media and grown overnight in a 30°C shaker incubator at 250 rpm. Once the yeast culture had reached a concentration of $8-9 \times 10^7$ cells mL⁻¹ the cells were spun down at 4000xg for 10 minutes at 4°C then washed with an equal volume of phosphate buffered saline (PBS) to cell mass. Cells were resuspended in an equal volume of lysis buffer (8 mM Na₂HPO₄, 2 mM NaH₂PO₄, 0.2 M NaCl, 1 mM phenylmethane sulfonyl fluoride (PMSF), 1 mM dithiothreitol (DTT), and 1% dimethyl sulfoxide (DMSO)) and lysed by

vortexing cells with 0.5 mm glass beads (1 mg beads per 1 mg cells) for 1 hour at 4°C. The lysate was separated from the beads then the beads were washed twice with 10 mL of lysis buffer to recover more lysate. The lysate was cleared of debris by centrifugation first at 4000xg, 4°C for 10 min, then at 45000xg, 4°C for 1 hour. The final supernatant was then incubated with 1 mL of 4-Aminophenyl- β -D-thiogalactopyranoside-Agarose 4B affinity beads (Sigma-Aldrich) overnight at 4°C with light rocking (~ 0.5 intervals sec^{-1}). After overnight incubation the lysate plus affinity bead slurry was run through a 10 mL polypropylene column (Thermo Scientific). The affinity beads collected in the column were then washed twice with 50 mL of wash buffer (8 mM Na_2HPO_4 , 2 mM NaH_2PO_4 , and 0.2 M NaCl). Elution was performed by incubation of the affinity beads with 5 mL volumes of elution buffer (0.1 M $\text{Na}_2\text{B}_4\text{O}_7$, pH 10.0) at 4°C for 1.5 hours in the capped column. Following the incubation period the eluent was ran through the column and collected. Concentration of the eluate and buffer exchange with PBS was performed using Ultracel-50K filter units (Amicon) and centrifugation at 4000xg, 4°C for 10 min. Further separation of the IL2RG -1 PRF:: β -GAL fusion protein from contaminating protein was accomplished by an 8% SDS-PAGE. A band at the expected size of 124 kDa was excised from the gel and sent to Dr. Yan Wang at the UMD Proteomics Core Facility for in-gel digestion and mass spectrometry analysis.

In-gel digestion of IL2RG -1:: β -GAL and peptide extraction

The polyacrylamide gel band at ~124 kDa was sliced to pieces of ~ 1 mm³ and de-stained by washing twice with 200 μ L 50% acetonitrile (ACN) in 50 mM Tetraethylammonium bromide (TEAB). Disulfide bridge reduction was performed by first dehydrating with 200 μ L of ACN then incubation in 200 μ L of 50 mM DTT in 50 mM TEAB at 55°C for 30 min. Alkylation was performed by dehydrating a second time with another 200 μ L ACN and then incubation with 200 μ L of 55 mM iodoacetamide (IAA) in 50 mM TEAB at room temperature in the dark for 60 min. Digestion of the protein in-gel was performed by dehydrating the gel again in 200 μ L ACN followed by incubation with 10 μ L of 200 ng/ μ L Glu-C (Promega) covered with 50 μ L 0.1 M TEAB at 35°C overnight. After the overnight digestion the aqueous solution containing solubilized peptides was collected. The gel fragment was then extracted first with 50 μ L of water and second with 50 μ L of a 70% ACN and 0.5% trifluoroacetic acid (TFA) solution. All extracts were combined and concentrated under vacuum to 10 μ L. This concentrate was then diluted with 50 μ L of Solvent A (2.5% ACN, 0.1% formic acid) and 2 μ L 10% TFA.

LC-MS/MS analysis of IL2RG -1PRF:: β -GAL fusion protein

20 μ L of the peptide sample was loaded into a 0.3 x 5 mm C18 PepMap 100 μ -precolumn (Thermo Scientific) and trapped at 5 μ L/ min with 100% Solvent A (2.5% ACN, 0.1% formic acid) before being eluted and separated by a 75 μ m x 25 cm Acclaim PepMap 100 nano column.. Elution was performed with a gradient of 2-40% Solvent B (70% ACN 0.1% formic acid) over 150 min.

Mass spectra were acquired with an Orbitrap Fusion Lumos mass spectrometer (Thermo Scientific) at a resolution of 120,000 ($m/z = 200$) with a scan range of 400-1600 m/z . Precursor ions with a positive charge of 2-7 and a signal intensity above 50,000 units were selected for MS/MS. Data dependent MS/MS was carried out with cycle times of 3 sec and dynamic exclusion (one repeat count after 20 seconds).

LC-MS/MS data analysis

The sequence of the IL2RG -1 PRF:: β -GAL fusion protein was added to a common contaminant database originally compiled by the Max Planck Institute of Biochemistry at Martinsried. The search for the trans-frame containing peptide was carried out using Sequest HT and Mascot search engines in the Proteome Discoverer (v. 2.0) program against the modified common contaminant database and the yeast protein database. The search was set to find peptides digested with Glu-C. Precursor mass tolerance was set to 20 ppm for the search but later filtered to 5 ppm in report. Fragment mass tolerance was set to 0.6 Da. Maximum of 1 missed cleavage was allowed in the search. Carbamidomethylation of cysteine was set as fixed modification. Deamidation of asparagine and glutamine, methionine oxidation, and protein N-terminal acetylation were set as variable modifications.

Appendix A: Table of oligonucleotides used for cloning, sequencing primers, and qPCR primers

Primer #	Oligonucleotide sequence (5'→3')	Oligonucleotide description
1	tcatacaaaatgacttctaggatcctcgagcattttcgcaagaagat gcacctgatgaaatgggaaaatataatcaaatcgttcggtgagcgagt tctcaaaaatgaacaaatgtcgacccccaaaatcggaggggcccctt ggggaggggctggggcctccccatgcaaccagcatagccccta ctgggccccccatgttacaccctaaagcctgaaaccggtaccgat cccgtcgttttacaacgctgt	Gblock used to create pjd1980
2	tcatacaaaatgacttctaggatcctcgagtcattttcgcaagaaga tgacctgtgaaatgggaaaatataatcaaatcgttcggtgagcgagt ctcaaaaatgaacaaatgtcgacaccaagaaaaattaaatgtg agttcaatcctgaaagttcctggactgccagattcataggggtgatg acattcaagctagagatgaagtggaaggttttctgcaagatacgttc ctcagcaaggatcctcaactccctgagctcggtagccgatcccgtc gt	Gblock used to create pjd1979
3	cgttgagcgagttctcaaaaatgaacaaatgtcgacccccaaactca ggggcctcgtctgtctccctagttccctctctgggctcccctcagacc agacccccagcttatgtcctgggctggccagtgacccccctggagc cccggatccccggggagctcatggaagacgccccaaaacataa agaaaggccccggcgccattc	Gblock used to create pjd2001
4	atcatacaaaatgacttctaggatcctcgagcattttcgcaagaag atgcacctgatgaaatgggaaaatataatcaaatcgttcggtgagcga gttctcaaaaatgaacaaatgtcgacaaaaaatgtgggtgagctgga ggctacttccgccttcttagcgtctggtcagagagctgatggatatcc catttgggtcccgacaagatgacatagattgcaaaaaggtagccgat cccgtcgttttacaacgctgt	Gblock used to create pjd1666
5	atcatacaaaatgacttctaggatcctcgagcattttcgcaagaag atgcacctgatgaaatgggaaaatataatcaaatcgttcggtgagcga gttctcaaaaatgaacaaatgtcgacgggaaaacaggggagggg gtgagggaaacccacgacgacccagcccggggaggccgggc tccgcaaagcgctactcccgtcagacaaacgaaggaatcgctac cgcaccggtaccgatcccgtcgttttacaacgctgt	Gblock used to create pjd1665
6	aaccaagggggtggttagt	Forward sequencing primer for pti25 inserts
7	attcaggctgcgcaactgtt	Reverse sequencing primer for pti25 inserts

8	atcatacaaaaatgacttctaggatcctcgagcattttcgcaagaag atgcacctgatgaaatgggaaaatatacaaatcggttcggtgagcga gttctcaaaaatgaacaaatgtcgacaaaaagaccagaagtgg actgtagaagaaagcgagtgggtcaaggctggagtgcagaaata tggggaaggaaactgggctgccatttctaaaaattaccattgttac aggtaccgatcccgtcgtttacaacgctgt	Gblock used to create pjd1533
9	gcgagttctcaaaaatgaacaaatgtcgactttttcttctgctgctctgt tggatcatctggcctgtgtgttatggaaaaaaggatta	Forward oligonucleotide used to create pjd1676
10	gctccccgggggatccgttccagagtcttcttatgatcggggagact gggccatacgataggcttaatcctttttccataacacacag	Reverse oligonucleotide used to create pjd1676
11	gcgagttctcaaaaatgaacaaatgtcgacaaaaaggagatcc acctctaccaaacattgtgttcagctccaggacccacgggaacc	Forward oligonucleotide used to create pjd1671
12	gctccccgggggatcccggatcaccagattctgcagtttagcatct gtgtggcctgtctcctgggtcccgtgggtcctggagc	Reverse oligonucleotide used to create pjd1671
13	gcgagttctcaaaaatgaacaaatgtcgacctaaccctcaaatcg gaggggcccttggggagggcctggggcctcccatgcaaccag c	Forward oligonucleotide used to create pjd1669
14	gagctccccgggtaggatccggttcaggcttaggggttaacatg ggggggcccagtaggggctatgctgggtcatggggaggcccc	Reverse oligonucleotide used to create pjd1670
15	catgagctccccgggggatccggttcaggcttaggggttaacatg ggggggcccagtaggggctatgctgggtcatggggaggcccc	Reverse oligonucleotide used to create pjd1667-1669
16	gcgagttctcaaaaatgaacaaatgtcgaccccaaatcggagg ggcccttggggagggcctggggcctcccatgcaaccagcata gc	Forward oligonucleotide used to create pjd1667 and pjd1670
17	ctcaaaaatgaacaaatgtcgacctaaccataaaatataatccgt gagttcaatcctgaaagttcctggactgccagattcataggg	Forward oligonucleotide used to create pjd1674

18	gttctcaaaaatgaacaaatgtcgacaaagaactgaatccgtgag ttcaatcctgaaagttcctggactgccagattcataggggtg	Forward oligonucleotide used to create pjd1673
19	gttctcaaaaatgaacaaatgtcgacaaaaattaaatccgtgag ttcaatcctgaaagttcctggactgccagattcataggggtg	Forward oligonucleotide used to create pjd1672
20	gctccccgggggatccgggaaacgtatcttgcagaaaacctcca ctcatctctagcttgaatgtcatccaccctatgaatctggcagt	Reverse oligonucleotide used to create pjd1672-pjd1674
21	gtgaggagaagtctgcgtcgacccccgaaggaggggcccttggg gaggggctggggcctccccatgcaaccagcatagcccctactgg g	Forward oligonucleotide used to create pjd1536
22	cccacagggcagtgaccaagcttgtggttcaggcttaggggtgaa catggggggcccagtaggggctatgctggttgcaggggagg	Reverse oligonucleotide used to create pjd1535 and pjd1536
23	gtgaggagaagtctgcgtcgaccccaaaaggaggggcccttggg gaggggctggggcctccccatgcaaccagcatagcccctactgg g	Forward oligonucleotide used to create pjd1535
24	ctcggfaccggggatcctctagactagtcccaaacagacagaa tggtgcatctgtccagtgaggagaagtctgcgtcgacgaagacgcc aaaaacaagcttggcactgccctgtggggcaaggtgaatgtgga agaagtgggtgtagggcctgggagggttggtatccttttacagca caactaatgagacagatagaaactggctttagaaacagagtag tcgctgctttctgccaggtgctgacttctcccctgggctgtttcatt tctcaggctgctggtgtctacccatggaccagaggttc	Gblock used to create pjd1534
25	gcaaccagcatagcccctactggcccccccatgttacacc	Forward oligonucleotide used to make pjd1542 and pjd2098
26	gggtgtaacatggggggggccagtaggggctatgctggttgc	Reverse oligonucleotide used to make pjd1542 and pjd2098

27	ggaggggcctggggactccccatgcaacc	Forward oligonucleotide used to make pjd1539 and pjd2095
28	ggttgcatggggagtccccaggcccctcc	Reverse oligonucleotide used to make pjd1539 and pjd2095
29	ccccgggggatccggttcaggtttaggggtgaacatgggggg	Reverse oligonucleotide used to create pjd1543
30	cccccatgttacaccctaaaacctgaaaccggatccccgggg	Forward oligonucleotide used to create pjd1543
31	ccggttcaggcttaggggtgaacatgagggggcccagtaggggc	Reverse oligonucleotide used to create pjd1541
32	gcccctactgggccccctcatgttacaccctaaagcctgaaaccgg	Forward oligo used to create pjd1541
33	ggggaggccccagaccctccccaaggg	Reverse oligonucleotide used to create pjd1540 and pjd2096
34	ccctggggaggggtctggggcctcccc	Forward oligonucleotide used to create pjd1540 and pjd2096
35	ggaggggcctggggcatccccatgcaaccagc	Forward oligonucleotide used to create pjd1538 and pjd2094
36	gctggttgcattggggatccccaggcccctcc	Reverse oligonucleotide used to create pjd1538 and pjd2094

37	ttctcaaaaatgaacaaatgtcgacccccgaagaaggaggggcct tggggaggggcctggggcctccccatgcaaccagcatagccccta	Forward oligonucleotide used to create pjd1544
38	atgagctccccgggggatccggttcaggctttaggggtgaacatgg gggggcccagtaggggctatgctggttgcatggggaggcccca	Reverse oligonucleotide used to create pjd1544
39	agaagaacggcatcaaggtga	Forward qpcr primer for egfp in pjd1033
40	cggactgggtgctcaggtag	Reverse qpcr primer for egfp in pjd1033
41	gtgaactgcacttgacaagc	Forward qpcr primer for rabbit beta-globin in pjd976 based plasmids
42	atgatgagacagcacaataaccag	Reverse qpcr primer for rabbit beta-globin in pjd976 based plasmids
42	cgtacgtgatgttcacc	Dual-luciferase multiple cloning site sequencing primer
43	gccctactgggccccctcatgttacaccctaaagcctgaaacc	Forward mutagenic oligonucleotide for making pjd2097
44	ggtttcaggctttaggggtgaacatgagggggcccagtaggggc	Reverse mutagenic oligonucleotide for making pjd2097
45	ccccatgttacaccctaaaacctgaaaccacaagcttggtc	Forward mutagenic oligonucleotide for making pjd2099

46	gaccaagcttggtggttcagggttttaggggtgaacatgggg	Reverse mutagenic oligonucleotide for making pjd2099
47	catagaagacaccgggaccgat	Forward sequencing primer for pjd976 based plasmids
48	cagtgatagagaacgtataacctttaggcgtgtacgggtgggc	Forward oligonucleotide used to destroy unique hindIII site in pTRE3G-BI
49	gcccaccgtacacgcctaaaggttatacgttctctatcactg	Reverse oligonucleotide used to destroy unique hindIII site in pTRE3G-BI
50	tcgaagcggccgcactttactagtcacaacgatcgcagaaggatc ccgtat gctagctttcccctgcagg	Forward oligonucleotide used to replace pTRE3G-BI MCS1 with new multiple cloning site
51	cctgcaggggaaagctagcatacgggatccttctgcatcgttgtga ctagtaaagtgcggccgct	Reverse oligonucleotide used to replace pTRE3G-BI MCS1 with new multiple cloning site
52	ctaggttaattaagcataagctactgggtgtatttaaadc	Forward oligonucleotide used to replace pTRE3G-BI MCS2 with new multiple cloning site

53	aattgatttaaatacaccagtacttatgcttaattaac	Reverse oligonucleotide used to replace pTRE3G-BI MCS2 with new multiple cloning site
54	ctgattatgatcctcctaggatttaaattacgaatggagagcgacga gagcggcctgcccgccatggagatcgagtgccgcatcaccggca ccctgaacggcgtggagttcgagctggtggcggaggagggc acccccgagcagggccgatgaccaacaagatgaagagcacc aaaggcgcctgaccttcagcccctacctgctgagccacgtgatgg gctacggcttctaccacttcggcacctaccccagcggctacgagaa ccccttctgcacgccatcaacaacggcggctacaccaacacccg catcgagaagtacgaggacggcggcgtgctgcacgtgagcttcag ctaccgctacgaggccggccgctgatcggcgacttcaaggtgat gggcaccggctccccgaggacagcgtgatcttcaccgacaagat catccgacgaacgccaccgtggagcacctgcacccatgggcg ataacgatctggatggcagcttcacccgcacctcagcctgcgcga cggcggctactacagctccgtggtggacagccacatgcacttcaa gagcgccatccaccccagcatcctgcagaacgggggccccatgtt cgcctccgcccgtggaggaggatcacagcaacaccgagctgg gcatcgtggagtaccagcacgcctcaagacccccggatgcagatg ccggtgaagaataacgcagttaattaacaattctccaggcgatctg a	Gblock used to add GFP into the pTRE3G-BI plasmid as part of the construction of pJD2106
55	catgggatagggattcgggt	Forward blunt end adapter ligated used to create an insertion site for a hygromycin resistance gene
56	accggaatccctatcc	Reverse blunt end adapter ligated used to create an insertion site for a hygromycin resistance gene
57	actgtcggtagccagatatacgcggtgacattgattattgac	Forward primer used to amplify the CMV promoter from pCDNA3.1

58	act gtc ctg cag gcc agt aag cag tgg gtt ctc tag	Reverse primer used to amplify the CMV promoter from pCDNA3.1
----	---	---

Table 2. Oligonucleotides used for cloning, sequencing primers, and qPCR primers

Appendix B: Table of plasmids made or used

Plasmid Number	Backbone plasmid	Description
pTI25	pSB3/pBR322 ⁷³	Yeast plasmid with <i>lacZ</i> and <i>LEU2</i>
pJD175f	p2luci ⁷⁴	p2luci Bicistronic dual-luciferase reporter read-through control (Reference)
pJD187.wt	pJD175f	HIV-1 -1 PRF signal in Dual-luciferase reporter used as a positive control
pJD1800	pJD175f	Homo sapiens IL2RG -1 PRF@1008 (NCBI ref # (NCBI ref # NM_000206.2) in Dual-luciferase reporter (contains an AA nucleotide spacer after slip-site to prevent reading into -1 PTC)
pJD976	pTRE-R β ⁷⁵	pTRE-R β from G. Brewer lab mRNA stability reporter read-through control (Reference)
pJD1035	pJD976	mRNA stability reporter -1 premature termination codon control ³⁰
pJD1033	pEGFP	pEGFP from Clontech
pJD1636	N/A	PSF-TEFI-TPI1-BETAGAL-URA3 - BETA GALACTOSIDASE YEAST PLASMID from Sigma (cat# OGS544-5UG)
pJD2034	pJD175f	Homo sapiens IL2RG -1 PRF@1008 (NCBI ref # NM_000206.2) in Dual-luciferase reporter (contains a TC nucleotide spacer after slip-site to prevent reading into -1 PTC)
pJD1980	pTI25	Homo sapiens IL2RG -1 PRF@1008 (NCBI ref # NM_000206.2) in β -galactosidase reporter
pJD1979	pTI25	Homo sapiens IL7RA -1 PRF@874 (NCBI ref # NM_002185.3) in β -galactosidase reporter
pJD2001	pJD175f	Homo sapiens CSF2RB (IL3RB) -1 PRF@2160 (NCBI ref # NM_000395.2) Dual-luciferase reporter
pJD1666	pTI25	Homo sapiens TERF2IP -1 PRF@1011 (NCBI ref # NM_018975.3) signal in β -galactosidase reporter
pJD1665	pTI25	Homo sapiens SMG6 -1 PRF@660 (NCBI ref # NM_017575) signal in β -galactosidase reporter
pJD1533	pTI25	Homo sapiens TERF2 -1 PRF@1461 (NCBI ref # NM_005652.4) in β -galactosidase reporter
pJD1676	pJD175f	Homo sapiens IL7RA -1 PRF@747 (NCBI ref # NM_002185.3) in dual-luciferase reporter
pJD1671	pJD175f	Homo sapiens IL2RG -1 PRF@354 (NCBI ref # NM_000206.2) in dual-luciferase reporter

pJD1669	pJD175f	Homo sapiens IL2RG -1 PRF@1008 (NCBI ref # NM_000206.2 out of frame control for pJD1667
pJD1670	pJD175f	Homo sapiens IL2RG -1 PRF@1008 (NCBI ref # NM_000206.2) -1 frame premature termination codon control for pJD1667
pJD1667	pJD175f	Homo sapiens IL2RG -1 PRF@1008 (NCBI ref # NM_000206.2) in pJD175f dual-luciferase reporter (re-cloned version of pJD1800)
pJD1668	pJD175f	Homo sapiens IL2RG -1 PRF@1008 (NCBI ref # NM_000206.2) silent-slip site mutant control for pJD1667
pJD1672	pJD175f	Homo sapiens IL7RA -1 PRF@874 (NCBI ref # NM_002185.3) in dual-luciferase reporter (different clone form pJD1800)
pJD1673	pJD175f	Homo sapiens IL7RA -1 PRF@874 (NCBI ref # NM_002185.3) silent-slip site mutant control for pJD1672
pJD1674	pJD175f	Homo sapiens IL7RA -1 PRF@874 (NCBI ref # NM_002185.3) out of frame control for pJD1672
pJD1675	pJD175f	Homo sapiens IL7RA -1 PRF@874 (NCBI ref # NM_002185.3) -1 frame premature termination codon control for pJD1672
pJD1536	pJD1534	Homo sapiens IL2RG -1 PRF@1008 (NCBI ref # NM_000206.2) silent slip-site mutant in exon 1 of β -globin
pJD1535	pJD1534	Homo sapiens IL2RG -1 PRF@1008 (NCBI ref # NM_000206.2) in exon 1 of β -globin
pJD1534	pJD976	Same as pJD976 except as restriction sites inserted into exon 1 of β -globin for cloning
pJD1538	pJD2034	Homo sapiens IL2RG -1 PRF@1008 (NCBI ref # NM_000206.2) with C→A (note that this was incorrectly cloned and should be a C→T) COSM3670280 mutation in pJD175f Dual-luciferase reporter
pJD1539	pJD2034	Homo sapiens IL2RG -1 PRF@1008 (NCBI ref # NM_000206.2) with C→A COSM1558340 mutation in pJD175f dual-luciferase reporter
pJD1540	pJD2034	Homo sapiens IL2RG -1 PRF@1008 (NCBI ref # NM_000206.2) with C→T COSM1124594 mutation in pJD175f dual-luciferase reporter
pJD1541	pJD2034	Homo sapiens IL2RG -1 PRF@1008 (NCBI ref # NM_000206.2) with C→T COSM3372325 mutation in pJD175f dual-luciferase reporter

pJD1542	pJD2034	Homo sapiens IL2RG -1 PRF@1008 (NCBI ref # NM_000206.2) with G→C COSM4110798 mutation in pJD175f dual-luciferase reporter
pJD1543	pJD2034	Homo sapiens IL2RG -1 PRF@1008 (NCBI ref # NM_000206.2) with G→A COSM1124593 mutation in pJD175f dual-luciferase reporter
pJD1544	pJD175f	Homo sapiens IL2RG -1 PRF@1008 (NCBI ref # NM_000206.2) silent slip-site mutant control for pJD2034
pJD2044	pJD175f	Same dual-luciferase reporter as pJD175f except that the SV40 promoter was exchanged with a full CMV promoter
pJD2075	pJD2044	Human IL2RG -1 PRF@1008 from start codon with C→A (note that this was incorrectly cloned and should be a C→T) mutation COSM3670280 (mRNA accession # is NM_000206.2) inserted into pJD2044 dual-luciferase reporter
pJD2076	pJD2044	Human IL2RG -1 PRF@1008 from start codon with C→A mutation COSM1558340 (mRNA accession # is NM_000206.2) inserted into pJD2044 dual-luciferase reporter
pJD2077	pJD2044	Human IL2RG -1 PRF@1008 from start codon with C→T mutation COSM1124594 (mRNA accession # is NM_000206.2) inserted into pJD2044 dual-luciferase reporter
pJD2078	pJD2044	Human IL2RG -1 PRF@1008 from start codon with C→T mutation COSM3372325 (mRNA accession # is NM_000206.2) inserted into pJD2044 dual-luciferase reporter
pJD2079	pJD2044	Human IL2RG -1 PRF@1008 from start codon with G→C mutation COSM4110798 (mRNA accession # is NM_000206.2) inserted into pJD2044 dual-luciferase reporter
pJD2080	pJD2044	Human IL2RG -1 PRF@1008 from start codon with G→A mutation COSM1124593 (mRNA accession # is NM_000206.2) inserted into pJD2044 dual-luciferase reporter
pJD2081	pJD2044	Human IL2RG -1 PRF@1008 from start codon with silent-slip site mutations (mRNA accession # is NM_000206.2) inserted into pJD2044 dual-luciferase reporter

pJD2094	pJD1535	Human IL2RG -1 PRF@1008 from start codon with C→A (note that this was incorrectly cloned and should be a C→T) mutation COSM3670280 (mRNA accession # is NM_000206.2) in pJD976 based beta-globin mRNA stability reporter
pJD2095	pJD1535	Human IL2RG -1 PRF@1008 from start codon with C→A mutation COSM1558340 (mRNA accession # is NM_000206.2) in pJD976 based beta-globin mRNA stability reporter
pJD2096	pJD1535	Human IL2RG -1 PRF@1008 from start codon with C→T mutation COSM1124594 (mRNA accession # is NM_000206.2) in pJD976 based beta-globin mRNA stability reporter
pJD2097	pJD1535	Human IL2RG -1 PRF@1008 from start codon with C→T mutation COSM3372325 (mRNA accession # is NM_000206.2) in pJD976 based beta-globin mRNA stability reporter
pJD2098	pJD1535	Human IL2RG -1 PRF@1008 from start codon with G→C mutation COSM4110798 (mRNA accession # is NM_000206.2) in pJD976 based beta-globin mRNA stability reporter
pJD2099	pJD1535	Human IL2RG -1 PRF@1008 from start codon with G→A mutation COSM1124593 (mRNA accession # is NM_000206.2) in pJD976 based beta-globin mRNA stability reporter
pJD2106	pTRE3G-BI from Clontech	New version of β-globin mRNA stability reporter. The test mRNA and normalization mRNA are expressed via the same promoter in this construct.
pJD2113	pJD2106	-1 PTC control for new version of β-globin mRNA stability reporter system. The β-globin from pJD1035 replaced the β-globin in pJD2106.
pJD2114	pJD2106	Homo sapiens IL2RG -1 PRF@1008 (NCBI ref # NM_000206.2) in exon 1 of β-globin within the new mRNA stability reporter pJD2106
pJD2115	pJD2106	Homo sapiens IL2RG -1 PRF@1008 (NCBI ref # NM_000206.2) silent slip-site mutant in exon 1 of β-globin within the new mRNA stability reporter pJD2106

pJD2116	pJD2106	Human IL2RG -1 PRF@1008 from start codon with C→A (note that this was incorrectly cloned and should be a C→T) mutation COSM3670280 (mRNA accession # is NM_000206.2) within exon 1 of β-globin in the new mRNA stability reporter pJD2106
pJD2117	pJD2106	Human IL2RG -1 PRF@1008 from start codon with C→A mutation COSM1558340 (mRNA accession # is NM_000206.2) within exon 1 of β-globin in the new mRNA stability reporter pJD2106
pJD2118	pJD2106	Human IL2RG -1 PRF@1008 from start codon with C→T mutation COSM1124594 (mRNA accession # is NM_000206.2) within exon 1 of β-globin in the new mRNA stability reporter pJD2106
pJD2119	pJD2106	Human IL2RG -1 PRF@1008 from start codon with C→T mutation COSM3372325 (mRNA accession # is NM_000206.2) within exon 1 of β-globin in the new mRNA stability reporter pJD2106
pJD2120	pJD2106	Human IL2RG -1 PRF@1008 from start codon with G→C mutation COSM4110798 (mRNA accession # is NM_000206.2) within exon 1 of β-globin in the new mRNA stability reporter pJD2106
pJD2121	pJD2106	Human IL2RG -1 PRF@1008 from start codon with G→A mutation COSM1124593 (mRNA accession # is NM_000206.2) within exon 1 of β-globin in the new mRNA stability reporter pJD2106

Table 3. Plasmids used and/or made

Appendix C: Table of yeast strains made or used

Strain ID	Genotype
yJD1370	MATa <i>trp1Δ his3 ura3 leu2 pep4::HIS3 nuc1::LEU2</i> K1 ⁻ L-A ⁻ L-BC ⁺
yJD1716	pJD1979 (<i>TRP1</i> selectable marker) transformed into yJD1370
yJD1717	pJD1980 (<i>TRP1</i> selectable marker) transformed into yJD1370
yJD1719	pJD1636 (<i>URA3</i> selectable marker) transformed into yJD1573
yJD1720	pJD1636 (<i>URA3</i> selectable marker) transformed into yJD1575
yJD1721	pJD1636 (<i>URA3</i> selectable marker) transformed into yJD1578
yJD1722	pJD1636 (<i>URA3</i> selectable marker) transformed into yJD1158
yJD1723	pJD1636 (<i>URA3</i> selectable marker) transformed into yJD1574
yJD1724	pJD1636 (<i>URA3</i> selectable marker) transformed into yJD1577
yJD1725	pJD1636 (<i>URA3</i> selectable marker) transformed into yJD1589
yJD1573	MAT α <i>his3-1; leu2-0; lys2-0; ura3-0</i> ; YGR214W::KanR (rpS0A deletion)
yJD1575	MAT α <i>his3-1; leu2-0; lys2-0; ura3-0</i> ; YCR031C::KanR (rps14A deletion)
yJD1578	MAT α <i>his3-1; leu2-0; lys2-0; ura3-0</i> ; YNL302C::KanR (rpS19B deletion)
yJD1158	(from ResGen) BY4742 MATalpha <i>his3D1 leu2D0 lys2D0 ura3D0</i> wild type Killer -
yJD1574	MAT α <i>his3-1; leu2-0; lys2-0; ura3-0</i> ; YLR048W::KanR (rps0B deletion)
yJD1577	MAT α <i>his3-1; leu2-0; lys2-0; ura3-0</i> ; YOL121C::KanR (rpS19A deletion)
yJD1589	MAT a <i>his3-1; leu2-0; lys2-0; met15-0; ura3-0</i> ; YJL191W::G418R (RPS14B deletion)
yJD1752	pTI25 (<i>TRP1</i> selectable marker) transformed into yJD1370

Table 4. Yeast strains used and/or made

Appendix D: Alignments of metazoan IL2RG sequences to Homo sapiens -1 PRF signals.

Figure 13. Alignment of metazoan IL2RG sequences to the Homo sapiens signal at 354.

Full length IL2RG sequences from the species listed above were aligned using Seaview64 software. Sequences were then trimmed down to only the sequence that aligned with the IL2RG -1 PRF signal at 354. The number above the sequences refers to the position from the start of the -1 PRF signal.

Homo_sapiens
 Pan_troglodytes
 Pan_paniscus_var_X1
 Pan_paniscus_var_X2
 Gorilla_gorilla
 Nomascus_leucogenys
 Macaca_millatta
 Cercopithecus_atys
 Chlorocebus_sabaeus
 Callithrix_jacchus
 Propithecus_cognareri
 Canis_lupus_familiaris
 Bos_taurus
 Phseter_catodon
 Chinchilla_lanigera
 Rattus_norvegicus
 Muntiacus_reevesi
 Pteropus_allecto
 Microtus_ochrogaster
 Monodelphis_domestica
 Sarcophilus_harrisii
 Piceodula_albicolis
 Anolis_carolinensis
 Chelonia_mydas
 Alligator_mussissippiensis
 Xenopus_tropicalis
 Takifugu_rubripes
 Gingivostoma_cirratum

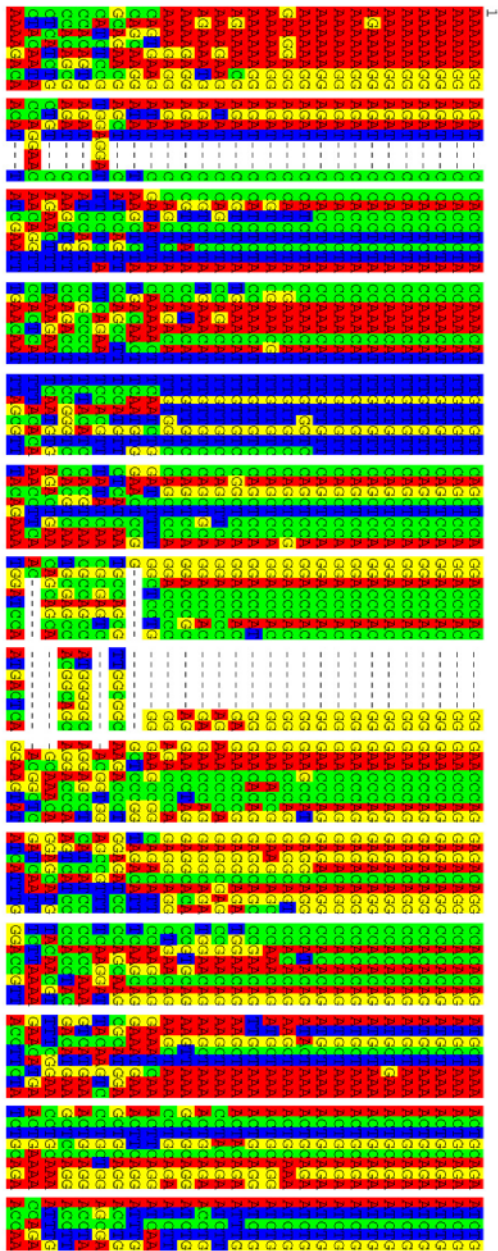
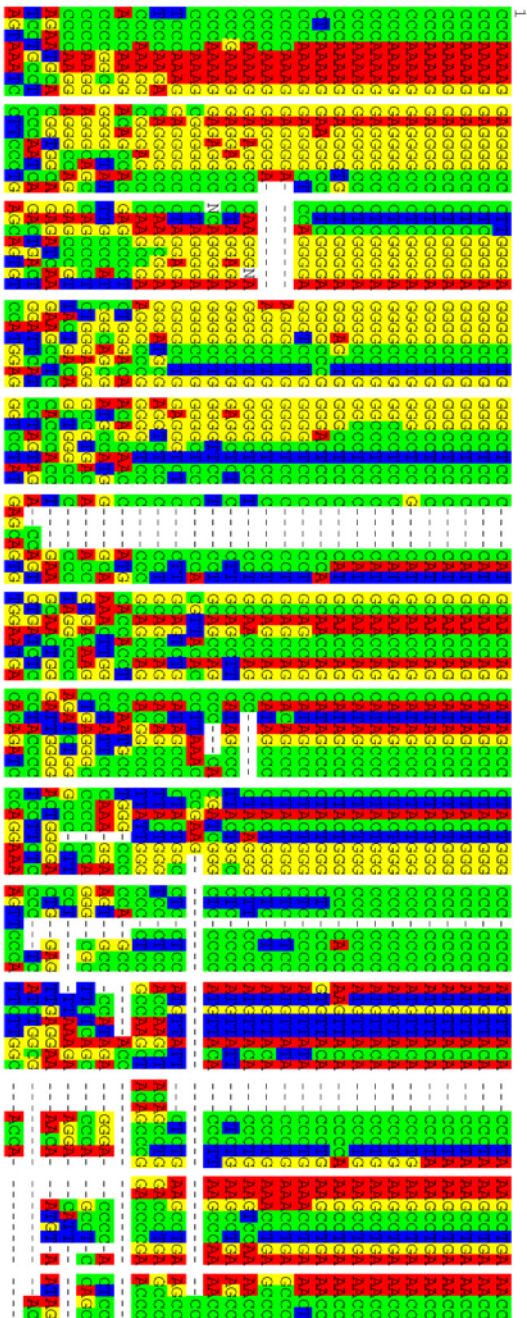


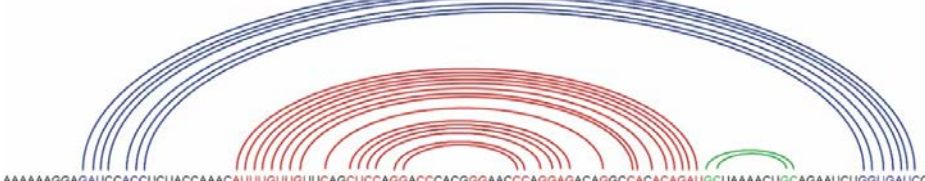
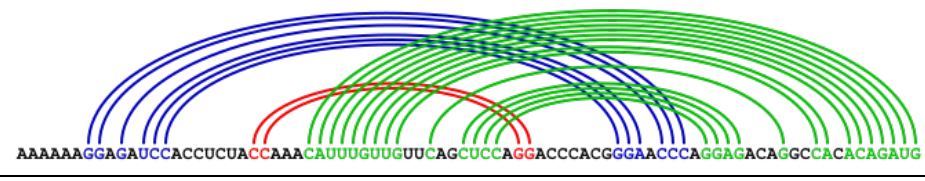
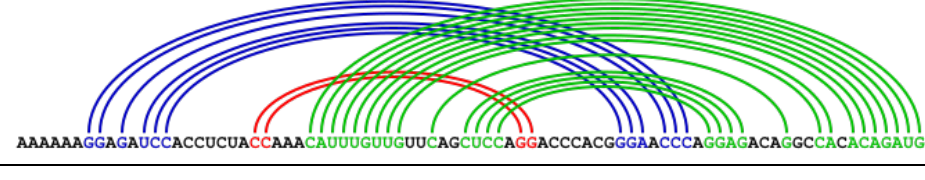
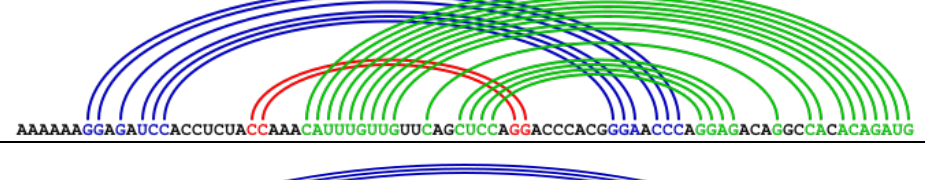
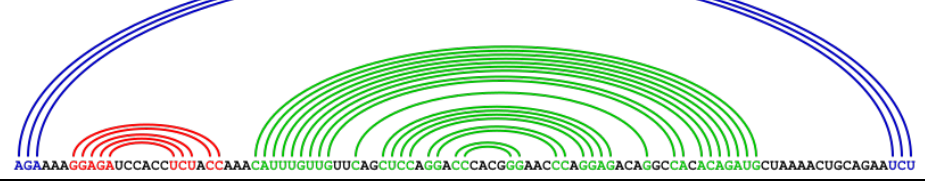
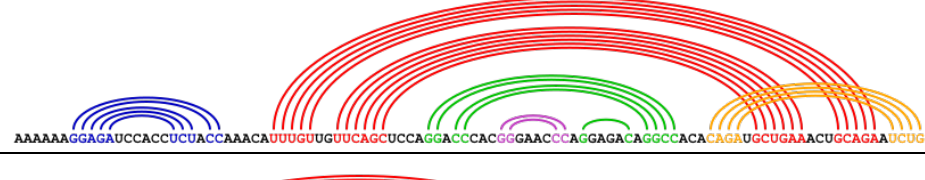
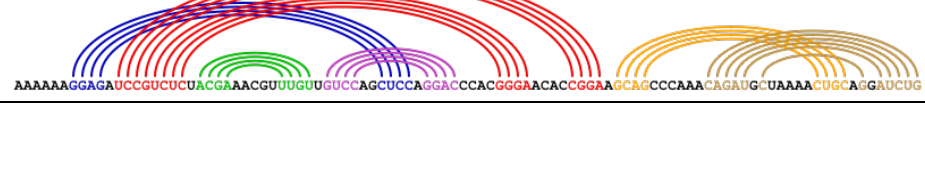
Figure 14. Alignment of metazoan IL2RG sequences to the Homo sapiens signal at 1008.

Full length IL2RG sequences from the species listed above were aligned using Seaview64 software. Sequences were then trimmed down to only the sequence that aligned with the IL2RG -1 PRF signal at 1008. The number above the sequences refers to the position from the start of the -1 PRF signal.

Homo_sapiens
 Pan_troglodytes
 Pan_paniscus_var_X1
 Pan_paniscus_var_X2
 Gorilla_gorilla
 Nomascus_leucogenys
 Macaca_mulatta
 Cercopithecus_atrys
 Chlorocebus_sabaeus
 Callithrix_jacchus
 Propithecus_coguerelli
 Canis_lupus_familiaris
 Bos_taurus
 Phylaxer_catodon
 Chinchilla_lanigera
 Rattus_norvegicus
 Miniopterus_natalensis
 Pteropus_allecto
 Microtus_ochrogaster
 Morodelphis_domestica
 Sarcophilus_harrisii
 Piceadula_albicollis
 Anolis_carolinensis
 Chelonis_mydas
 Alligator_mississippiensis
 Xenopus_tropicalis
 Takifugu_rubripes
 Ginglymostoma_citratum



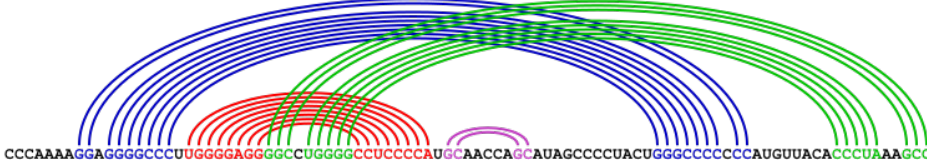
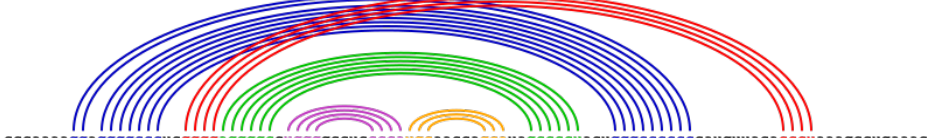
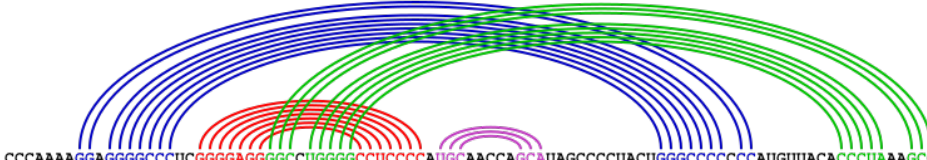
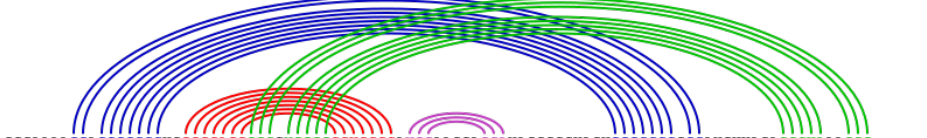
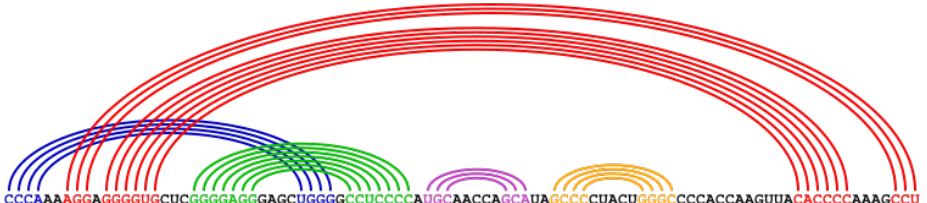
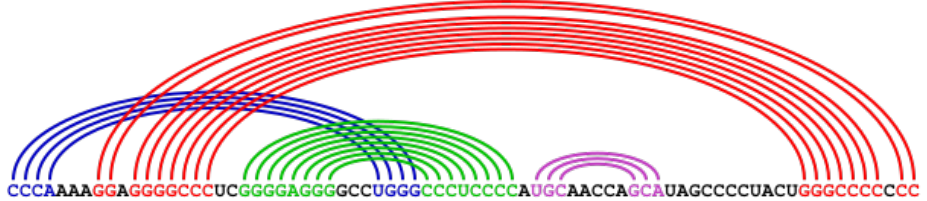
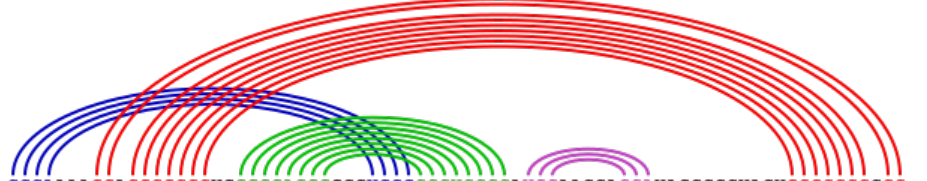
Appendix E: Table of hotknots folding solutions for mammalian sequences that align with Homo sapiens IL2RG -1 PRF signal at 354.

<p><i>Homo sapiens</i> MFE = -22.84</p>	
<p><i>Pan paniscus</i> MFE = -21.54</p>	
<p><i>Gorilla gorilla</i> MFE = -21.54</p>	
<p><i>Callithrix jacchus</i> MFE = -21.54</p>	
<p><i>Macaca mulatta</i> MFE = -21.60</p>	
<p><i>Nomascus leucogenys</i> MFE = -25.30</p>	
<p><i>Bos tauros</i> MFE = -27.20</p>	

<p><i>Physeter catodon</i> MFE = -25.40</p>	
<p><i>Rattus norvegicus</i> MFE = -18.50</p>	
<p><i>Chinchilla lanigera</i> MFE = -20.30</p>	
<p><i>Canis lupus familiaris</i> MFE = -25.20</p>	
<p><i>Miniopterus natelensis</i> MFE = -21.80</p>	
<p><i>Pteropus Alecto</i> MFE = -25.25</p>	
<p><i>Monodelphis domestica</i> MFE = -23.51</p>	

Table 5. Hotknots folding solutions for mammalian sequences that align with Homo sapiens IL2RG -1 PRF signal at 354.

Appendix F: Table of nupack solutions for mammalian sequences that align with Homo sapiens IL2RG -1 PRF signal at 1008.

<p><i>Homo sapiens</i> MFE = -46.70</p>	
<p><i>Pan troglodytes</i> MFE = -34.66</p>	
<p><i>Pan paniscus</i> MFE = -34.66</p>	
<p><i>Gorilla gorilla</i> MFE = -34.66</p>	
<p><i>Callithrix jacchus</i> MFE = -41.30</p>	
<p><i>Cercocebus atys</i> MFE = -45.90</p>	
<p><i>Macaca mulatta</i> MFE = -45.90</p>	

<p><i>Nomascus leucogenys</i> MFE = -43.80</p>	
<p><i>Bos tauros</i> MFE = -36.30</p>	
<p><i>Physeter catodon</i> MFE = -36.30</p>	
<p><i>Rattus norvegicus</i> MFE = -38.30</p>	
<p><i>Canis lupis familiaris</i> MFE = -43.61</p>	
<p><i>Monodelphis domestica</i> MFE = -38.30</p>	
<p><i>Sarcophilus harrisii</i> MFE = -47.80</p>	

Table 6. Nupack folding solutions for mammalian sequences that align with *Homo sapiens* IL2RG -1 PRF signal at 1008.

Bibliography

1. Crick, F. Central Dogma of Molecular Biology. *Nature* **227**, 561–563 (1970).
2. Schmeing, T. M. & Ramakrishnan, V. What recent ribosome structures have revealed about the mechanism of translation. *Nature* **461**, 1234–1242 (2009).
3. Lafontaine, D. L. & Tollervey, D. The function and synthesis of ribosomes. *Nat. Rev. Mol. Cell Biol.* **2**, 514–20 (2001).
4. Nirenberg, M. Historical review: Deciphering the genetic code - A personal account. *Trends Biochem. Sci.* **29**, 46–54 (2004).
5. Sonenberg, N. & Hinnebusch, A. G. Regulation of Translation Initiation in Eukaryotes: Mechanisms and Biological Targets. *Cell* **136**, 731–745 (2009).
6. Hinnebusch, A. G. The scanning mechanism of eukaryotic translation initiation. *Annu. Rev. Biochem.* **83**, 779–812 (2014).
7. Kozak, M. Initiation of translation in prokaryotes and eukaryotes. *Gene* **234**, 187–208 (1999).
8. Hershey, J. W. B. Protein phosphorylation controls translation rates. *J. Biol. Chem.* **264**, 20823–20826 (1989).
9. Lehmann, J. & Libchaber, A. Degeneracy of the genetic code and stability of the base pair at the second position of the anticodon. *RNA* **14**, 1264–9 (2008).
10. Blanchard, S. C., Gonzalez, R. L., Kim, H. D., Chu, S. & Puglisi, J. D.

- tRNA selection and kinetic proofreading in translation. *Nat. Struct. Mol. Biol.* **11**, 1008–1014 (2004).
11. Leung, E. K. Y., Suslov, N., Tuttle, N., Sengupta, R. & Piccirilli, J. A. The Mechanism of Peptidyl Transfer Catalysis by the Ribosome. *Annu. Rev. Biochem.* **80**, 527–555 (2011).
 12. Berry, M. J., Banu, L., Harney, J. W. & Larsen, P. R. Functional characterization of the eukaryotic SECIS elements which direct selenocysteine insertion at UGA codons. *EMBO J.* **12**, 3315–22 (1993).
 13. Nakamura, Y. & Ito, K. tRNA mimicry in translation termination and beyond. *Wiley Interdiscip. Rev. RNA* **2**, 647–668 (2011).
 14. Mitkevich, V. A. *et al.* Termination of translation in eukaryotes is mediated by the quaternary eRF1-eRF3-GTP-Mg²⁺ complex. The biological roles of eRF3 and prokaryotic RF3 are profoundly distinct. *Nucleic Acids Res.* **34**, 3947–3954 (2006).
 15. Baranov, P. V., Gesteland, R. F. & Atkins, J. F. Recoding: Translational bifurcations in gene expression. *Gene* **286**, 187–201 (2002).
 16. Belew, A. T., Hepler, N. L., Jacobs, J. L. & Dinman, J. D. PRFdb: a database of computationally predicted eukaryotic programmed -1 ribosomal frameshift signals. *BMC Genomics* **9**, 339 (2008).
 17. Jacks, T., Madhani, H. D., Masiarz, F. R. & Varmus, H. E. Signals for ribosomal frameshifting in the rous sarcoma virus gag-pol region. *Cell* **55**, 447–458 (1988).
 18. Dinman, J. D. Mechanisms and Implications of Programmed

- Translational Frameshifting. *Wiley Interdiscip. Rev. RNA* **3**, 661–673 (2013).
19. Harger, J. W., Meskauskas, A. & Dinman, J. D. An ‘integrated model’ of programmed ribosomal frameshifting. *Trends Biochem. Sci.* **27**, 448–454 (2002).
 20. Yu, C. H., Noteborn, M. H., Pleij, C. W. A. & Olsthoorn, R. C. L. Stem-loop structures can effectively substitute for an RNA pseudoknot in -1 ribosomal frameshifting. *Nucleic Acids Res.* **39**, 8952–8959 (2011).
 21. Liao, P. Y., Choi, Y. S., Dinman, J. D. & Lee, K. H. The many paths to frameshifting: Kinetic modelling and analysis of the effects of different elongation steps on programmed -1 ribosomal frameshifting. *Nucleic Acids Res.* **39**, 300–312 (2010).
 22. Namy, O., Moran, S. J., Stuart, D. I., Gilbert, R. J. C. & Brierley, I. A mechanical explanation of RNA pseudoknot function in programmed ribosomal frameshifting. *Nat. Lett.* **441**, 244–247 (2006).
 23. Léger, M., Dulude, D., Steinberg, S. V. & Brakier-Gingras, L. The three transfer RNAs occupying the A, P and E sites on the ribosome are involved in viral programmed -1 ribosomal frameshift. *Nucleic Acids Res.* **35**, 5581–5592 (2007).
 24. Dulude, D., Berchiche, Y. A., Gendron, K., Brakier-Gingras, L. & Heveker, N. Decreasing the frameshift efficiency translates into an equivalent reduction of the replication of the human immunodeficiency virus type 1. *Virology* **345**, 127–136 (2006).

25. Plant, E. P., Rakauskaitė, R., Taylor, D. R. & Dinman, J. D. Achieving a golden mean: mechanisms by which coronaviruses ensure synthesis of the correct stoichiometric ratios of viral proteins. *J. Virol.* **84**, 4330–4340 (2010).
26. Shigemoto, K. *et al.* Identification and characterisation of a developmentally regulated mammalian gene that utilises -1 programmed ribosomal frameshifting. *Nucleic Acids Res.* **29**, 4079–4088 (2001).
27. Wills, N. M., Moore, B., Hammer, A., Gesteland, R. F. & Atkins, J. F. A functional -1 ribosomal frameshift signal in the human paraneoplastic Ma3 gene. *J. Biol. Chem.* **281**, 7082–7088 (2006).
28. Jacobs, J. L., Belew, A. T., Rakauskaitė, R. & Dinman, J. D. Identification of functional, endogenous programmed - 1 ribosomal frameshift signals in the genome of *Saccharomyces cerevisiae*. *Nucleic Acids Res.* **35**, 165–174 (2007).
29. Belew, A. T., Advani, V. M. & Dinman, J. D. Endogenous ribosomal frameshift signals operate as mRNA destabilizing elements through at least two molecular pathways in yeast. *Nucleic Acids Res.* **39**, 2799–2808 (2011).
30. Belew, A. T. *et al.* Ribosomal frameshifting in the CCR5 mRNA is regulated by miRNAs and the NMD pathway. *Nature* **512**, 265–269 (2014).
31. Advani, V. M., Belew, A. T. & Dinman, J. D. Yeast telomere

maintenance is globally controlled by programmed ribosomal frameshifting and the nonsense-mediated mRNA decay pathway.

Translation **1**, e24418 (2013).

32. Zhang, S. *et al.* Polysome-associated mRNAs are substrates for the nonsense-mediated mRNA decay pathway in *Saccharomyces cerevisiae*. *RNA* **3**, 234–244 (1997).
33. Brogna, S. & Wen, J. Nonsense-mediated mRNA decay (NMD) mechanisms. *Nat. Struct. Mol. Biol.* **16**, 107–113 (2009).
34. Gaba, A., Jacobson, A. & Sachs, M. S. Ribosome occupancy of the yeast CPA1 upstream open reading frame termination codon modulates nonsense-mediated mRNA decay. *Mol. Cell* **20**, 449–460 (2005).
35. Sun, X. *et al.* Nonsense-mediated decay of mRNA for the selenoprotein phospholipid hydroperoxide glutathione peroxidase is detectable in cultured cells but masked or inhibited in rat tissues. *Mol. Biol. Cell* **12**, 1009–1017 (2001).
36. Kertész, S. *et al.* Both introns and long 3'-UTRs operate as cis-acting elements to trigger nonsense-mediated decay in plants. *Nucleic Acids Res.* **34**, 6147–6157 (2006).
37. Kebaara, B. W. & Atkin, A. L. Long 3'-UTRs target wild-type mRNAs for nonsense-mediated mRNA decay in *Saccharomyces cerevisiae*. *Nucleic Acids Res.* **37**, 2771–2778 (2009).
38. Franks, T. M., Singh, G. & Lykke-Andersen, J. Upf1 ATPase-dependent mRNP disassembly is required for completion of nonsense-mediated

- mRNA decay. *Cell* **143**, 938–950 (2010).
39. Swisher, K. D. & Parker, R. Interactions between Upf1 and the Decapping Factors Edc3 and Pat1 in *Saccharomyces cerevisiae*. *PLoS One* **6**, e2657 (2011).
 40. Mitchell, P. & Tollervey, D. An NMD Pathway in Yeast Short Article Involving Accelerated Deadenylation and Exosome-Mediated 3'→5' Degradation. *Mol. Cell* **11**, 1405–1413 (2003).
 41. Eberle, A. B., Lykke-Andersen, S., Muhlemann, O. & Jensen, T. H. SMG6 promotes endonucleolytic cleavage of nonsense mRNA in human cells. **16**, 49–55 (2009).
 42. Schell, T. *et al.* Complexes between the nonsense-mediated mRNA decay pathway factor human upf1 (up-frameshift protein 1) and essential nonsense-mediated mRNA decay factors in HeLa cells. *Biochem. J.* **373**, 775–783 (2003).
 43. Fiorini, F., Le Hir, H. & Boudvillain, M. Tight intramolecular regulation of the human Upf1 helicase by its N- and C-terminal domains. **41**, 2404–2415 (2013).
 44. Kashima, I. *et al.* Binding of a novel SMG-1–Upf1–eRF1–eRF3 complex (SURF) to the exon junction complex triggers Upf1 phosphorylation and nonsense-mediated mRNA decay. *Genes Dev.* **20**, 355–367 (2006).
 45. Yamashita, A. *et al.* SMG-8 and SMG-9 , two novel subunits of the SMG-1 complex , regulate remodeling of the mRNA surveillance

complex during nonsense-mediated mRNA decay. 1091–1105 (2009).
doi:10.1101/gad.1767209.exhibit

46. Jonas, S., Weichenrieder, O. & Izaurralde, E. An unusual arrangement of two 14-3-3-like domains in the SMG5–SMG7 heterodimer is required for efficient nonsense-mediated mRNA decay. *Genes Dev.* **27**, 211–225 (2013).
47. Ishigaki, Y. *et al.* Evidence for a Pioneer Round of mRNA Translation: mRNAs Subject to Nonsense-Mediated Decay in Mammalian Cells Are Bound by CBP80 and CBP20. **106**, 607–617 (2001).
48. Wang, J., Gudikote, J. P., Olivas, O. R. & Wilkinson, M. F. Boundary-independent polar nonsense-mediated decay. *EMBO Rep.* **3**, 274–279 (2002).
49. Metze, S., Herzog, V. A., Ruepp, M. & Mühlemann, O. Comparison of EJC-enhanced and EJC-independent NMD in human cells reveals two partially redundant degradation pathways. *RNA* **19**, 1432–1448 (2013).
50. Behm-Ansmant, I., Gatfield, D., Rehwinkel, J. & Izaurralde, E. A conserved role for cytoplasmic poly(A)-binding protein 1 (PABPC1) in nonsense-mediated mRNA decay. *EMBO J.* **26**, 1591–1601 (2007).
51. Celik, A., Kervestin, S. & Jacobson, A. NMD: At the crossroads between translation termination and ribosome recycling. *Biochimie* **114**, 2–9 (2015).
52. Noguchi, M. *et al.* Interleukin-2 Receptor gamma Chain Mutation Results in X-Linked Severe Combined Immunodeficiency in Humans.

- Cell* **73**, 147–157 (1993).
53. Matthews, D. J. *et al.* Function of the Interleukin-2 (IL-2) Receptor γ -Chain in Biologic Responses of X-Linked Severe Combined Immunodeficient B Cells to IL-2, IL-4, IL-13, and IL-15. *Blood* **85**, 38–42 (1995).
 54. Ginn, S. L. *et al.* A novel splice-site mutation in the common gamma chain (γ chain) gene IL2RG results in X-linked severe combined immunodeficiency with an atypical NK⁺ phenotype. *Hum Mutat* **23**, 522–523 (2004).
 55. Disanto, J. P., Mullert, W., Guy-grand, D., Fischer, A. & Rajewsky, K. Lymphoid development in mice with a targeted deletion of the interleukin 2 receptor γ chain. **92**, 377–381 (1995).
 56. Asao, H. *et al.* Cutting edge: the common gamma-chain is an indispensable subunit of the IL-21 receptor complex. *J Immunol* **167**, 1–5 (2001).
 57. Amorosi, S. *et al.* The cellular amount of the common γ -chain influences spontaneous or induced cell proliferation. *J. Immunol.* **182**, 3304–3309 (2009).
 58. Woods, N.-B., Bottero, V., Schmidt, M., von Kalle, C. & Verma, I. M. Gene therapy: therapeutic gene causing lymphoma. *Nature* **440**, 1123 (2006).
 59. Orr, S. J. *et al.* Implications for Gene Therapy-Limiting Expression of IL-2R γ C Delineate Differences in Signaling Thresholds Required for

- Lymphocyte Development and Maintenance. *J. Immunol.* **185**, 1393–1403 (2010).
60. Waickman, A. T., Park, J. Y. & Park, J. H. The common gamma-chain cytokine receptor: Tricks-and-treats for T cells. *Cell. Mol. Life Sci.* **73**, 253–269 (2016).
61. Hong, C. *et al.* Activated T Cells Secrete an Alternatively Spliced Form of Common gamma-Chain that Inhibits Cytokine Signaling and Exacerbates Inflammation. *Immunity* **40**, 910–923 (2014).
62. Suzuki, K. *et al.* Janus kinase 3 (Jak3) is essential for common cytokine receptor γ chain (γ c)-dependent signaling: comparative analysis of γ c, Jak3, and γ c and Jak3 double-deficient mice. *Int. Immunol.* **12**, 123–32 (2000).
63. Hofmann, S. R. *et al.* Jak3-Independent Trafficking of the Common gamma Chain Receptor Subunit: Chaperone Function of Jaks Revisited. *Mol. Cell. Biol.* **24**, 5039–5049 (2004).
64. Farabaugh, P. J. Programmed Translational Frameshifting. *Microbiol. Rev.* **60**, 103–134 (1996).
65. Lindeboom, R. G. H., Supek, F. & Lehner, B. The rules and impact of nonsense-mediated mRNA decay in human cancers. *Nat. Genet.* **48**, 1–9 (2016).
66. Garneau, N. L., Wilusz, J. & Wilusz, C. J. The highways and byways of mRNA decay. *Nat. Rev. Mol. Cell Biol.* **8**, 113–126 (2007).
67. Andrade, L. J. de O. *et al.* Association Between Hepatitis C and

- Hepatocellular Carcinoma. *J. Glob. Infect. Dis.* **1**, 33–37 (2009).
68. Mackall, C. L., Fry, T. J. & Gress, R. E. Harnessing the biology of IL-7 for therapeutic application. *Nat. Rev. Immunol.* **11**, 330–342 (2011).
 69. Goswami, R. & Kaplan, M. H. A Brief History of IL-9. *J. Immunol.* **186**, 3283–3288 (2011).
 70. Jabri, B. & Abadie, V. IL-15 functions as a danger signal to regulate tissue-resident T cells and tissue destruction. *Nat. Rev. Immunol.* **15**, 771–83 (2015).
 71. Spolski, R. & Leonard, W. J. Interleukin-21: a double-edged sword with therapeutic potential. *Nat. Rev. Drug Discov.* **13**, 379–95 (2014).
 72. Jacobs, J. L. & Dinman, J. D. Systematic analysis of bicistronic reporter assay data. *Nucleic Acids Res.* **32**, e160 (2004).
 73. Imura, T. & Toh-E, A. A cis-Acting Locus Needed for Stable Maintenance of the Yeast Plasmid pSB3. *Agric. Biol. Chem.* **54**, 2239–2246 (1990).
 74. Grentzmann, G., Ingram, J. A., Kelly, P. J., Gesteland, R. F. & Atkins, J. F. A dual-luciferase reporter system for studying recoding signals. *RNA* **4**, 479–86 (1998).
 75. Ysla, R. M., Wilso, G. M. & Brewer, G. Assays of Adenylate Uridylate-Rich Element-Mediated mRNA Decay in Cells. *Methods Enzymol.* **449**, 47–71 (2008).